ORKUSTOFNUN
NATIONAL ENERGY AUTHORITY
GEOTHERMAL DIVISION

Ingi Ólafsson
Karl Gunnarsson

THE JAN MAYEN RIDGE

Velocity structure from analysis of sonobuoy data

OS-89030/JHD-04
Reykjavík, August 1989

ORKUSTOFNUN
NATIONAL ENERGY AUTHORITY
GEOTHERMAL DIVISION

GRENSÁSVEGUR 9,
108 REYKJAVÍK ICELAND

Ingi Ólafsson
Karl Gunnarsson

THE JAN MAYEN RIDGE

Velocity structure from analysis of sonobuoy data

OS-89030/JHD-04
Reykjavík, August 1989

Abstract

We present the analysis of seismic refraction data (sonobuoy recordings) from the Norwegian-Icelandic seismic survey of the Jan Mayen Ridge, carried out in 1985. This entire project has been conducted in cooperation between the relevant institutions, Oljedirektoratet and Orkustofnun. The ridge is believed to be a fragment of continental crust, and the purpose of the survey was to map the sedimentary formations on the ridge. Over 40 sonobuoy profiles were analysed. The velocity structure of the main ridge block is in accordance with the assumption that the ridge is a continental fragment. The velocities of the Tertiary sediments on the ridge are comparable to those of the Tertiary sediments on the Norwegian margin, although higher velocities are found at the deeper part of the sequence on the Jan Mayen Ridge. No velocity structures comparable to the Cretaceous sequence on the Norwegian margin are observed on the ridge. Under the considerable pile of Tertiary sediments and Early Tertiary lavas, on the main ridge block, high-velocity sediments of presumably pre-Cretaceous age are present. In the east flank of the ridge, in the area of the transition between the oceanic and the continental crust, the thickness of the rocks in the velocity range 5-6 km/s increases abruptly. The nature and origin of this sequence is not known, but we belive it could be interpreted as some sort of transitional crust.

Contents

Figure captions.

Figure 1. Profile location. The main geological structures are from Skogseid and Eldholm (1987).

Figure 2. A type section of the northern part of the Jan Mayen Ridge (from NPD/OS report, in preparation). The section is based on reflection profile JM-11-85 (see figure 1 for location).

Figure 3. Sonobuoy profile 32 from the oceanic crust east of the Jan Mayen Ridge.

Figure 4. Sonobuoy profile 29 from the east flank of the ridge.

Figure 5. Sonobuoy profile 11 shot parallel to the strike on the top of the ridge.

Figure 6. An example of a sonobuoy profile from the Jan Mayen Basin to the west of the ridge.

Figure 7. The interpretation process of a sonobuoy data. The inversion can be done either in the tau-p or the x-t domain, but the modeling is usually done in the x-t domain.

Figure 8. An example of a comparison of observed and calculated traveltime curves. Solid curves are calculated traveltimes and dots are measured values.

Figure 9. Comparison of various inversion results and the modeled velocity function for sonobuoy profile 11.

Figure 10. The velocity as a function of depth for the profiles in the area of the oceanic crust east of the Jan Mayen Ridge. The arrows point to the JO horizon. See figure 1 for location.

Figure 11. The velocity as a function of depth for the profiles in the area of the dipping sequence in the east flank of the ridge and also in the area between the dipping sequence and the main ridge block. The arrows point to the horizon JO. See figure 1 for location.

Figure 12. The velocity structure below the main ridge block. The arrows point to the horizon JO. See figure 1 for location.

Figure 13. The velocity solutions for sonobuoy profiles 1 and 2 located in the southern part of the ridge (figure 1). The arrows point to the horizon JO.

Figure 14. Solutions of sonobuoy profiles in the Jan Mayen Basin.

Figure 15. Isovelocity curves along line JM-2. Dots mark the depth to horizon JO. The number of the profiles used to draw the curves are shown by small numbers.

Figure 16. Isovelocity curves along line JM-8. Dots mark the depth to horizon JO. WDR: Wedges of Dipping Reflectors. M: Moho

Figure 17. Isovelocity curves along line JM-11. Notations the same as in figures 15 and 16. The heavy black streak in the left part of the figure represents the opaque layer in the Jan Mayen Basin.

Figure 18. Isovelocity curves along line JM-14. Notation the same as in figures 15 and 16.

Figure 19. Typical velocity structure for the Møre Basin obtained from ESP data (Ólafsson, 1988).

Figure 20. The solutions of the sonobuoy data from the Jan Mayen Ridge area can be divided into two main groups, i.e. the main ridge block and the area of the dipping sequences and the area further east. The solutions were adjusted such that the depth to JO coincides.

Figure 21. Velocity structure below JO from the area to the east of the main block of the Jan Mayen Ridge compared with solutions of ESP profiles from oceanic crust off the Møre margin (from Ólafsson, 1988).

Figure 22. Velocity structure below JO on the main ridge block of the Jan Mayen Ridge compared with the velocity structure below Base Cretaceous of the Møre Basin. The solutions of the ESP data are adjusted such that Base Cretaceous coincides with the depth to JO.

Figure 23. a) A line drawing of reflection profile JM-11-85. b) Isovelocity curves along JM-11-85 plotted as functions of two-way traveltime.

Figure 24. Isovelocity cross section of the Jan Mayen Ridge (line JM-11-85) compared to the Møre margin (the Møre margin section is from Ólafsson, 1988).

1. Introduction

1.1 Location and purpose of work

In 1985, a marine geophysical survey was carried out in the area of the Jan Mayen Ridge in the Norwegian-Greenland Sea. In this survey, which was a joint project of the governments of Iceland and Norway, about 4000 km of multichannel seismic reflection profiles were shot. Simultaneously 44 sonobuoys were deployed, six of which never did work. Gravity and magnetic data were also obtained along profile lines. Profile locations are shown in figure 1. The first results of the survey have been published by Guðlaugsson et al. (1988). In this report we present the final results of the interpretation of the sonobuoy data. This work was arranged as a special cooperative effort by Oljedirektoratet of Norway (NPD) and Orkustofnun of Iceland (OS), the national institutes responsible. The interpretation was carried out at Orkustofnun, which provided facilities, while NPD provided financial support for a specialist for six months. The main objective was to map the velocity distribution in the deeper pre-Tertiary strata of the ridge, below the so-called horizon JO.

The Jan Mayen Ridge is a submarine ridge that runs to the south from Jan Mayen Island. The ridge can be divided into two main parts, a northern part and a southern part, separated by the Jan Mayen Trough (figure 1). The trough is about 30 km wide and 2000 m deep trending southwest-northeast. The northern part appears as a single north-south trending, flat=topped topographic ridge block, which can be followed southward, from Jan Mayen Island to 67.9°N, 11.5°W (figure 1). At about 69.0°N the trend of the ridge changes to a northeast-southwest direction. The water depth over the top increases from north to south with an average depth slightly less than 1000 m. The water depth increases rapidly to the east and the west of the ridge. To the west, in the Jan Mayen Basin, the seafloor is smooth and the water depth greater than 2000 m. The basin is separated from the Jan Mayen Trough by a southwestern extension of the Jan Mayen Ridge (figure 1). To the east the water depth gradually increases towards the deep Norway Basin. The southern part consists of many smaller topographic ridges that are seen as far south as 66.8°N. The ridges, which trend between north and northeast, rise to within 1000 m of the sea surface from the general topographic level of about 1600 m below the sea surface.

1.2 Previous works

Johnson and Heezen (1967) were the first to consider geophysical data from the Norwegian-Greenland Sea. They noted that the main Jan Mayen Ridge block represents a magnetic quiet zone. Therefore, they suggested the ridge to be a microcontinental fragment. Since then, the magnetic anomalies in the Norwegian-Greenland Sea have been studied in more detail, i.e. Talwani and Eldholm (1977), Nunns (1983), Vogt et al. (1980). These studies showed that the seafloor spreading axis had shifted westward once or twice. The spreading started just before the anomaly 24 time on the Aegir Ridge in the Norway Basin. Talwani and Eldholm (1977) noted that anomalies younger than anomaly 20 formed a fan-shaped pattern wider in its northern end than in the southern. They suggested that at the same time a complementary spreading took place in the area south of the Jan Mayen Ridge, thereby creating the eastern part of the Jan Mayen Ridge complex. On the other hand, Nunns (1983) and Larsen (1988) suggested that a fan-shaped spreading occurred on the southern part of the Kolbeinsey Ridge. Aegir Ridge was active until a time just before anomaly 7, but then the spreading center shifted to the west and the Jan Mayen Ridge split from Greenland. Vogt et al. (1970) noticed that the Kolbeinsey Ridge lies closer to the Greenland shelf edge than to the Jan Mayen Ridge. Therefore, they postulated an additional region of spreading on the eastern part of the Iceland Plateau. Later Vogt et al. (1980) rejected the existence of this extinct spreading axis.

Few regional multichannel seismic reflection surveys have been carried out in the Jan Mayen Ridge area (Gairaud et al. (1978), Navrestad and Jørgensen (1979), Ólafsson (1983), Skogseid and Eldholm (1987), Guðlaugsson et al. (1988)). Figure 2, from a NPD/OS report (in preparation), shows a generalized cross section of the main ridge block. This section is based on reflection line JM-11-85; see figure 1 for location. At a depth of a few hundred meters an unconformity is observed. Gairaud et al. (1978) named this horizon A, but to distinguish this from the Norwegian margin Skogseid and Eldholm (1987) named this reflector JA. The sediments above JA are horizontally stratified on the top of the ridge, but to the east the reflector dips eastward and the sediment thickness increases. Three drill-holes from the DSDP leg 38 were located on the top of the ridge. The results showed that the sediments above JA extend from Middle Miocene to Upper-Middle Oligocene in age, and the sediments below the

unconformity, which were drilled, range in age from Early Oligocene to Late Eocene (Talwani and Udintsev, 1976). At a greater depth on the ridge proper, another reflector, called horizon O by Gairaud et al. (1978) and JO by Skogseid and Eldholm (1987), was observed. This reflector is affected by many faults, most of them trending north-south. Gairaud et al. (1978) interpreted this reflector as representing crystalline basement. In later studies this reflector has been interpreted as Early Tertiary basalt flows (Ólafsson (1983), Nunns (1983), Skogseid and Eldholm (1987), Guðlaugsson et al. (1988)). The new seismic reflection data from 1985 (Guðlaugsson et al., 1988) show several reflectors below JO, in some cases down to a depth of 7 sec. However, the new data do not give a clear answer concerning the nature and origin of these reflectors.

In the area of the east flank of the ridge the sediment thickness above JO increases and reaches a maximum of about 2 sec twt (two way traveltime). Below reflector JO, wedges of dipping reflectors are observed. These reflectors are the counterparts of the seaward dipping reflectors observed on the outer Møre margin and Vøring Plateau off Norway. Dipping reflectors are observed along the entire east flank of the Jan Mayen Ridge (figure 1). However, they are not as clear and well developed as on the Norwegian margin. In many cases, the sub-basement reflectors are not typical seaward dipping as on the Norwegian margin; rather, they appear as an irregular sub-basement reflection pattern. There has been some disagreement as to the nature and origin of the dipping reflector sequence. However, the ODP leg 104 drilling results showed that the dipping sequence on the Vøring Plateau consists of series of tholeiitic basalt flows and interbedded volcaniclastic series (Eldholm, Thiede, Taylor et al., 1987). The drilling results did not answer the question whether the basalts rest on continental or oceanic crust. However, most observers agree that the dipping reflectors were formed in the first phase of seafloor spreading.

The western flank of the ridge is fault controlled and characterized by large rotated fault blocks. Dipping reflectors, of the same origin as those on the east flank, are not observed here. It seems as the eastern flank of the ridge is typical volcanic margin with sub-basement dipping reflectors and thick crust. The western flank, on the other hand, is typical non-volcanic margin characterized by rotated fault blocks as a result of crustal stretching when the ridge split from East Greenland just before anomaly 7

time.

The Jan Mayen Basin, to the west of the Jan Mayen Ridge, is characterized by a strong intrasedimentary reflector, which is called the opaque layer (Talwani and Eldholm, 1977). The nature of this layer (reflector) is not known, but most observers interpret it as a basaltic layer underlain by sediments.

Myhre et al. (1984) summarized results of available refraction data from the Jan Mayen Ridge. Beneath the main ridge block, average refractor velocities of 1.8, 2.2, 2.7, 3.1, 3.9, and 5.5 km/s were computed. However, the 2.7 km/s refractor was not observed where the water depth is less than 1.1 km. They suggested that the 5.5 km/s refractor represented an eastward dipping basement surface. They found velocities in the range 1.7-2.0 km/s to be typical for the sediments above reflector JA and 2.2-3.3 km/s for the unit between reflector JA and JO. Hinz and Schluter (1979) found the average velocity below JO to be in the range 4.0-4.5 km/s, whereas Gairaud et al. (1978) found it to be about 4.5 km/s. Myhre et al. (1984) suggested the refractor 3.9 km/s to be associated with JO and the 5.5 km/s refractor to originate below JO. Johansen et al. (1988) reported results of interpretation of an ESP profile located on the top of the main ridge block, between the location of sonobuoys 11 and 12 (figure 1). They found the velocity to be close to 4.0 km/s below JO. Johansen et al. (1988) concluded that the velocity structure below JO was comparable to the velocity structure of the Cretaceous sediments on the Norwegian margin.

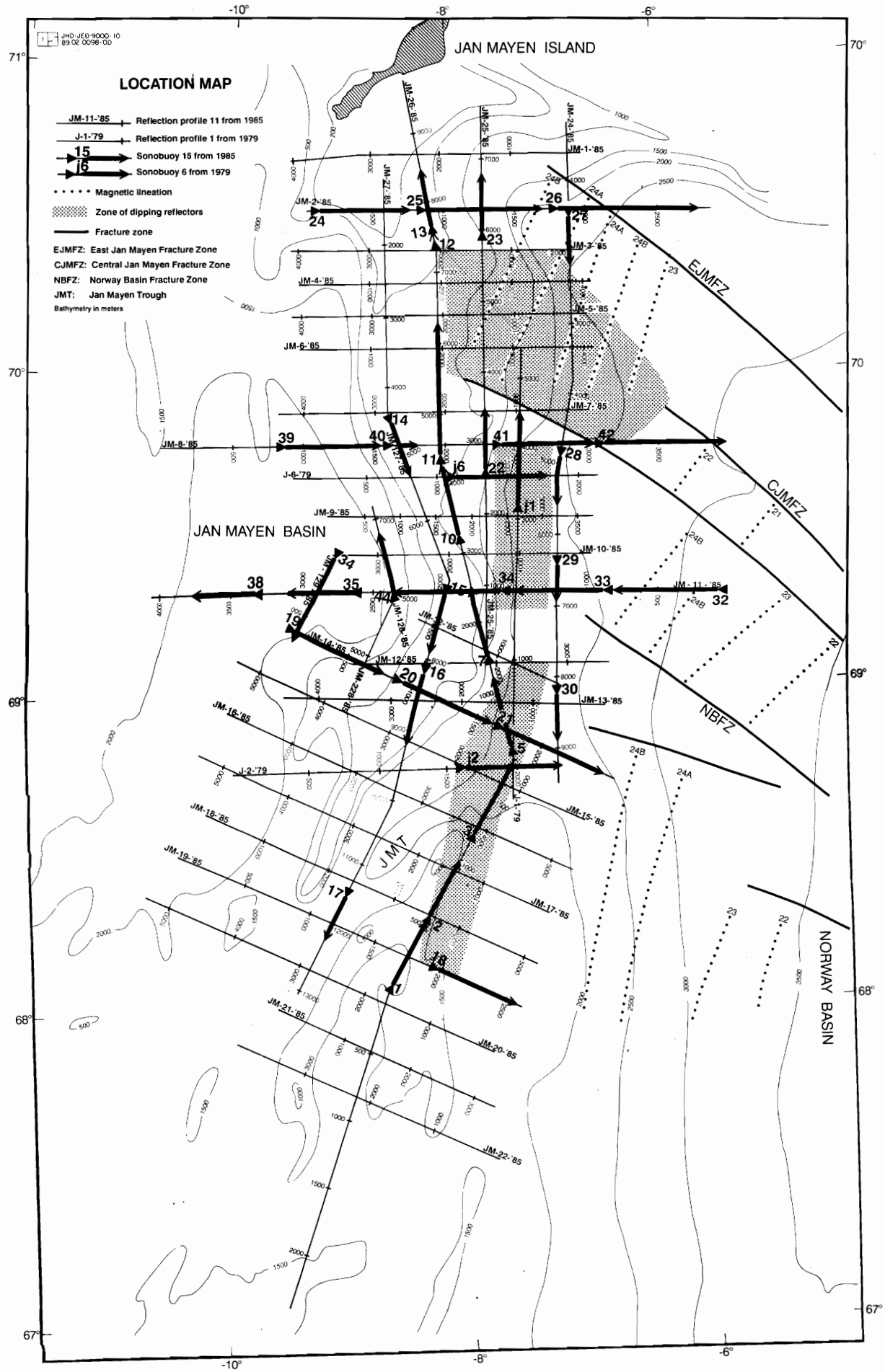
LOCATION MAP
JM-11-'85 Reflection profile 11 from 1985
J-1-'79 Reflection profile 1 from 1979
15 Sonobuoy 15 from 1985
j6 Sonobuoy 6 from 1979
Magnetic lineation
Zone of dipping reflectors
Fracture zone
EJMFZ: East Jan Mayen Fracture Zone
CJMFZ: Central Jan Mayen Fracture Zone
NBFZ: Norway Basin Fracture Zone
JMT: Jan Mayen Trough
Bathymetry in meters
JAN MAYEN ISLAND
JAN MAYEN BASIN
NORWAY BASIN
EJMFZ
CJMFZ
NBFZ
JMT
-10°
-8°
-6°
71°
70°
69°
68°
67°

Figure 1

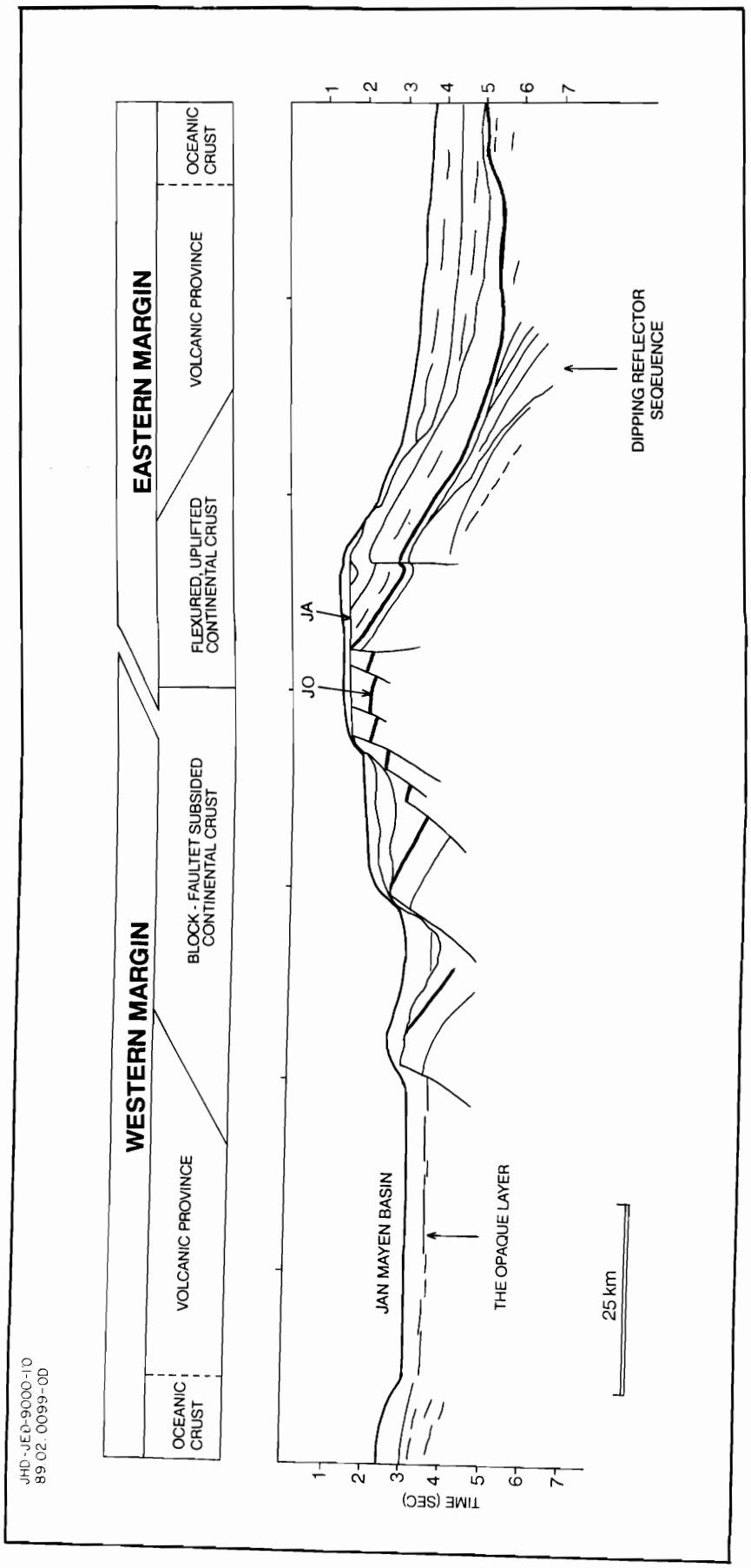
WESTERN MARGIN
EASTERN MARGIN
OCEANIC CRUST
VOLCANIC PROVINCE
BLOCK - FAULTET SUBSIDED CONTINENTAL CRUST
FLEXURED, UPLIFTED CONTINENTAL CRUST
VOLCANIC PROVINCE
OCEANIC CRUST
JA
JO
JAN MAYEN BASIN
THE OPAQUE LAYER
DIPPING REFLECTOR SEQEUENCE
25 km
TIME (SEC)
1
2
3
4
5
6
7
JHD-JED-9000-10
89 02 0099-00

Figure 2

2. Data

2.1 Data quality

The location of the sonobuoys is shown in figure 1. The quality of the data is in most cases very good. However, it is difficult to interpret some of the profiles because of topography and complicated geological structures. The study area can be divided into three sub-areas: (i) the east flank of the ridge, (ii) the main ridge block, and (iii) the Jan Mayen Basin.

(i) The east flank

The oldest part of the oceanic crust in the Norwegian-Greenland Sea is located in the easternmost part of this area. The area also contains the dipping reflector sequence and the transition between the oceanic crust and the assumed continental crust of the Jan Mayen Ridge. The sonobuoy profiles located in the area are all of very good quality. However, some of them were shot in an east-west direction and therefore crossed many important geological structures. Furthermore, the dip of the interfaces varies along the profile line. Therefore, the interpretation of these data can be difficult. The profiles shot in north-south direction are much easier to interpret. In most cases the recording time was only 8 sec along the north-south lines, however, so that the velocity structure in the deeper part of the crust was not obtained. Figure 3 shows an example of a very good sonobuoy data from the oceanic crust in the easternmost part of the area, sonobuoy 32. Strong first arrivals are observed out to a range of about 40 km. At distances over 18 km a second arrival is observed (shown by arrows in figure 3), which we interpret as a reflection from Moho, or possibly as a deep intracrustal reflector. Figure 4 shows an example of a profile (sonobuoy 29) where arrivals were only recorded to a range of about 20 km because of too short a record length.

(ii) The main ridge block

The Jan Mayen Ridge is affected by many faults that have a similar trend as the ridge, i.e. north-south in the northern part and northeast-southwest in the southern part (Guðlaugsson et al, 1988). Some of the sonobuoy peofiles were shot perpendicular to the faults, causing disturbances in the first arrival and, therefore, making the

interpretation difficult. On the other hand, the profiles shot parallel to the faults are of good quality, e.g. sonobuoy 11 (figure 5) where strong arrivals are observed out to a range of about 40 km. Also, second arrivals are observed at ranges over 18 km.

(iii) The Jan Mayen Basin

It is difficult to map the Jan Mayen Basin with the seismic method. This is because of the opaque layer. Figure 6 shows an example of a sonobuoy profile (sonobuoy 38) from the Jan Mayen Basin. Refraction arrivals from the opaque layer are observed in the range 5-8 km, but then the amplitude decreases abruptly. Another arrival is observed in the distance range of 7-10 km, with traveltimes of 5.8-6.5 sec. This is an indication of a low velocity layer below the opaque layer. Refraction arrivals corresponding to the first one on sonobuoy profile 38 are not observed on profiles 35 and 39. The reason may be that the opaque layer is too thin in this area to carry refracted waves for some kilometers.

2.2 Data analysis

The sonobuoy data and the reflection data were collected simultaneously. The sonobuoy data were recorded on one of the channels of the DFS V system. During processing of the reflection data, which was done by Geco A/S, the sonobuoy data were copied to separate tapes. Before plotting the data a filter test was made. The best results were obtained by using a 5-30 Hz band-pass filter. When scaling the data an AGC with a 1000 msec window was used. At Orkustofnun we attempted to enhance arrivals from the deeper part of the crust by using a velocity filter. The filtering did not improve the data significantly. In some cases, weak arrivals at far ranges were observed. These arrivals most likely represent refractions, diving waves, or wide angle reflections from the deeper part of the crust. We were able to enhance these arrivals by mixing traces along lines having similar dip as the arrivals. The mixing only strengthened arrivals that were seen as a weak trend, but "new" arrivals were not observed after the mixing.

In the interpretation of sonobuoy data one is interested in obtaining the velocity structure of the crustal layers. The interpretation process is shown in figure 7. The

first stage is an inversion that gives a velocity model. This model is then used as a starting model in the forward modeling process in which synthetic traveltime curves are calculated. These curves and the data are plotted to the same scale, and the traveltimes are compared. If the comparison shows too large a discrepancy, the velocity model is changed and new traveltime curves are calculated. This process is continued until a satisfactory accordance is achieved. Figure 8 shows an example of modeling of sonobuoy profile J2. The solid curves are the calculated traveltime curves while the dots are the observed traveltimes.

Many different inversion methods exist, and the inversion can be performed in the x-t, x-p, or tau-p domain. In the last few years, the tau-p method has been introduced in velocity inversion. In this method, the data are first transformed from the distance-traveltime (x-t) domain to the tau-p domain, where tau is the intercept time and p the ray parameter. There are many advantages to mapping traveltime data in the tau-p domain. The data are much better organized and easier to interpret in tau-p than in x-t. Diebold and Stoffa (1981) showed that all the post-critically reflected arrivals and also refracted waves and diving waves form, in the tau-p domain, a single monotonic curve containing all the information necessary to obtain a velocity-depth function. The inversion of the tau-p data is done by the use of the so-called tau-sum method. This method, described by Diebold and Stoffa (1981), is equivalent to the standard first arrival slope-intercept method, except that it is valid for all critical and post-critical arrivals, without distinction between reflections and refractions. A disadvantage of the tau-p method is that it only works on data from horizontally stratified media.

In the x-t domain the reflected waves and the refracted or diving waves are interpreted separately. The crustal velocities can be found from the refractions or the diving waves by using the well known slope-intercept or Wiechert-Herglotz methods. A very effective method, developed by Mykkeltveit (1980), gives the interval velocity from the reflected arrivals when the velocity structure in the layers above is known. The method is as follows: An arrival – at range x_1 and time t_1 – is identified as a reflection from the bottom of a layer. By ray tracing one can obtain a set of v-h (velocity-depth) points for different angles of emergence, and a v-h curve may be drawn. Next, another point (x_2,t_2) on the same reflection curve is picked, and the

same calculations are performed. This results in another v-h curve, and the crossing point for two such curves gives the actual thickness and velocity of the layer in question.

The quality of the data is variable so that in some cases reflections are clearly observed while refracted or diving waves are not, and also the other way around. Inversion of the reflections gives the average velocity in the layer, while the diving waves give the velocity gradient (if present). As a result, the "same" layer can be seen as a constant velocity layer in one sonobuoy profile but as a gradient layer in another profile. One must keep this in mind when comparing solutions of different profiles.

In the forward modeling algorithm used in the present study only plane layer interfaces, with or without dip, are allowed. Some of the profiles were shot in an east-west direction on the eastern slope of the ridge where the dip of the interfaces varies along the profile. This results in an inaccurate velocity function, e.g. sonobuoy 18. Furthermore, although the dip can be measured from the reflection profile it does not necessarily mean that this is the dip that should be used in the modeling. This is because velocities in rocks, especially in sediments, increase with increasing depth of burial. However, in most cases the plane layer interfaces are a very good approximation. Figure 9 shows a comparison between inversion solutions and forward modeling of sonobuoy profile 11. The agreement is very good, especially in the upper part of the crust.

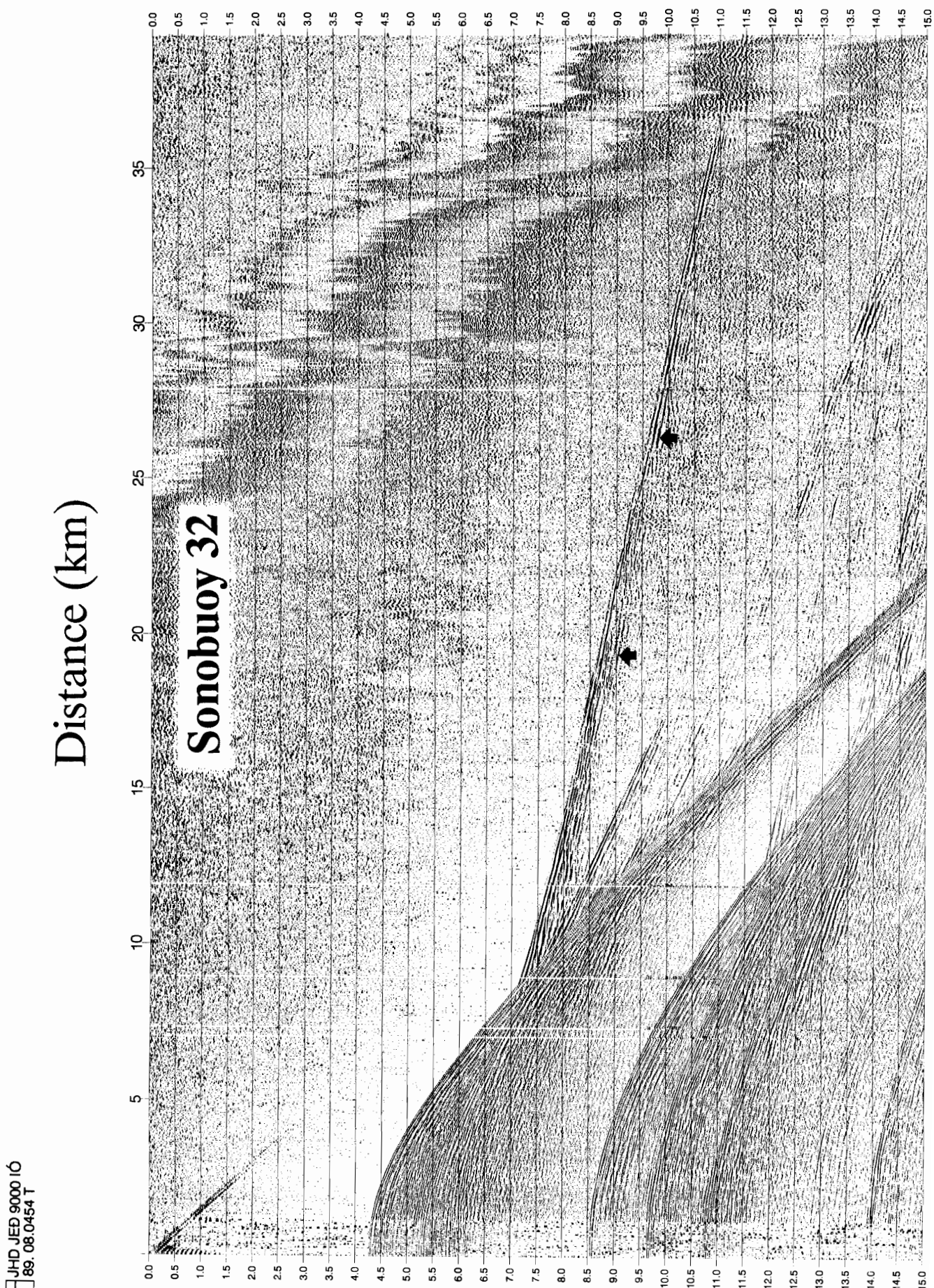
Sonobuoy 32
Distance (km)
Traveltime (sec)
JHD JED 9000 IÓ
89. 08.0454 T

Figure 3

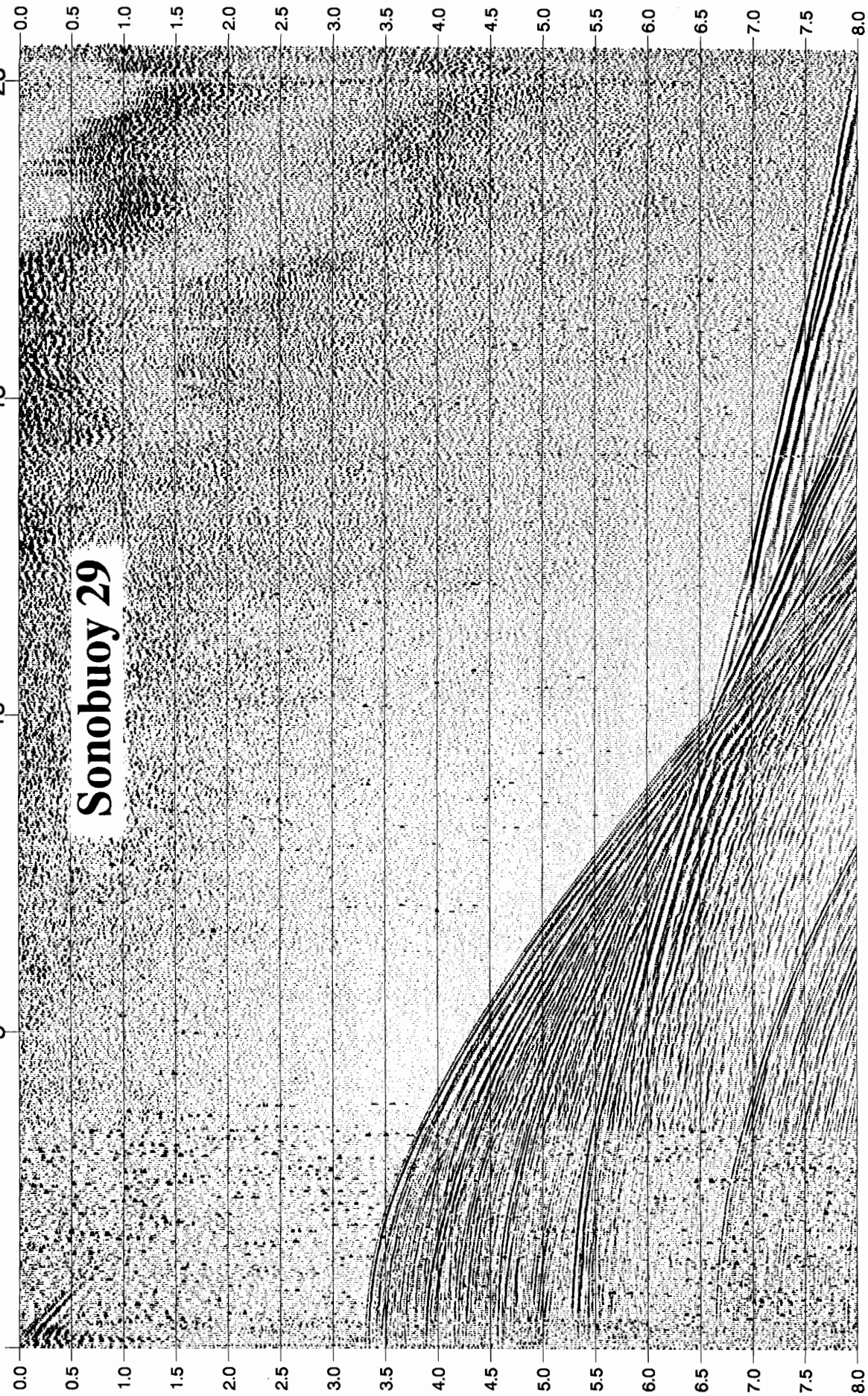

JHD JED 90000 IÓ
89. 08.0455 T

Figure 4

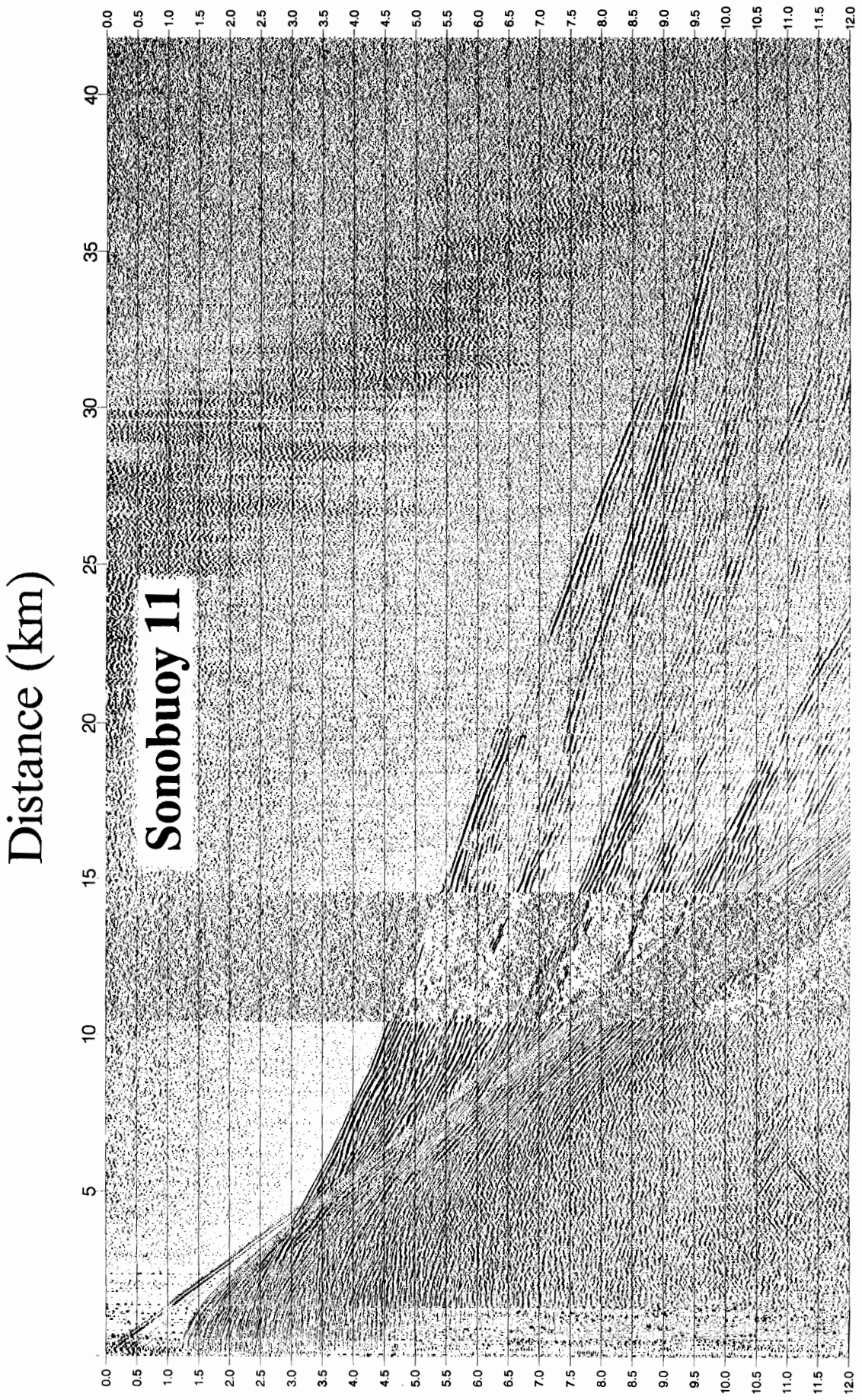

JHD JED 9000 IÓ
89. 08.0456 T

Figure 5

JHD JED 9000 IÓ
89. 08.0457 T

Figure 6

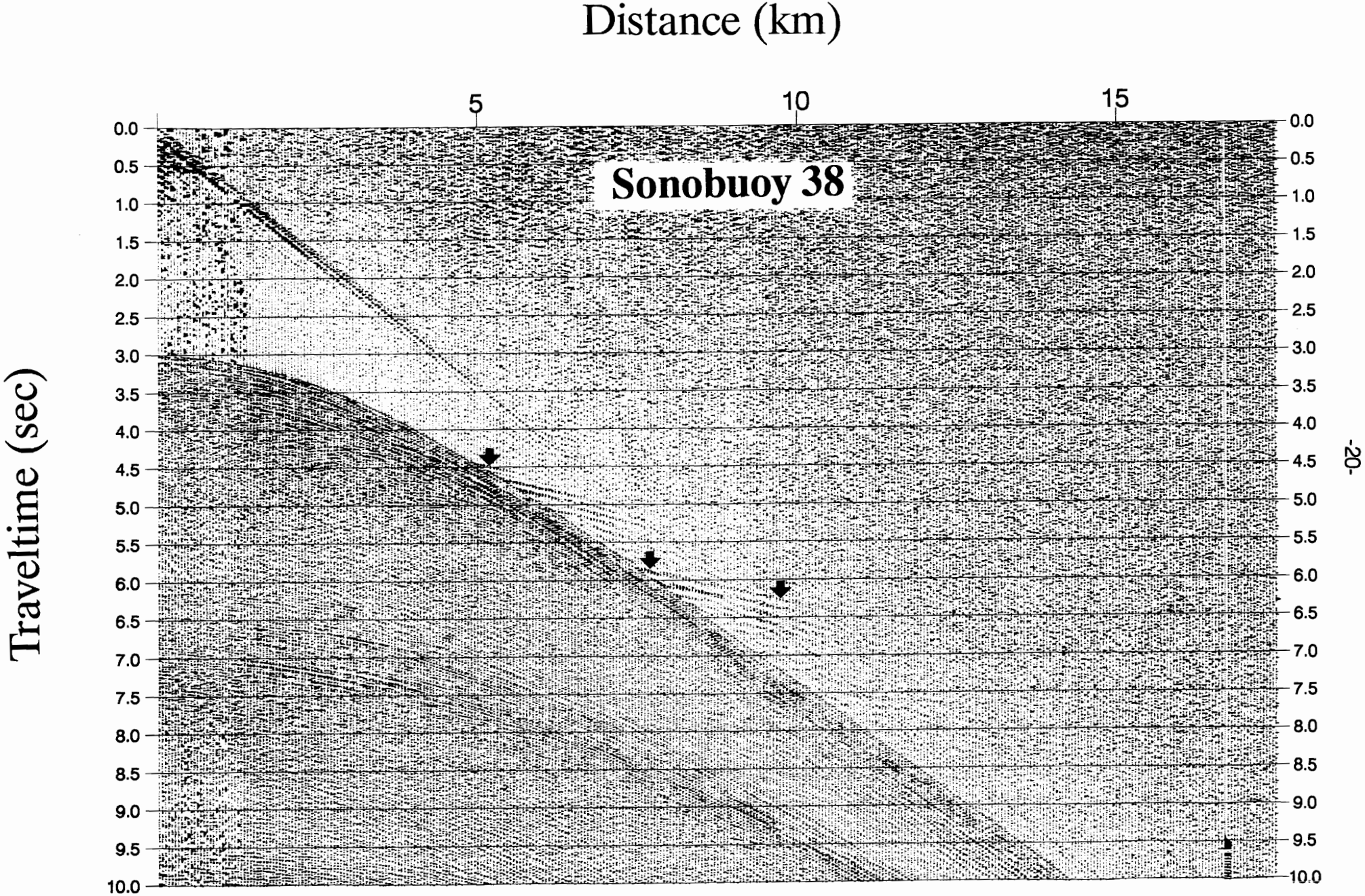

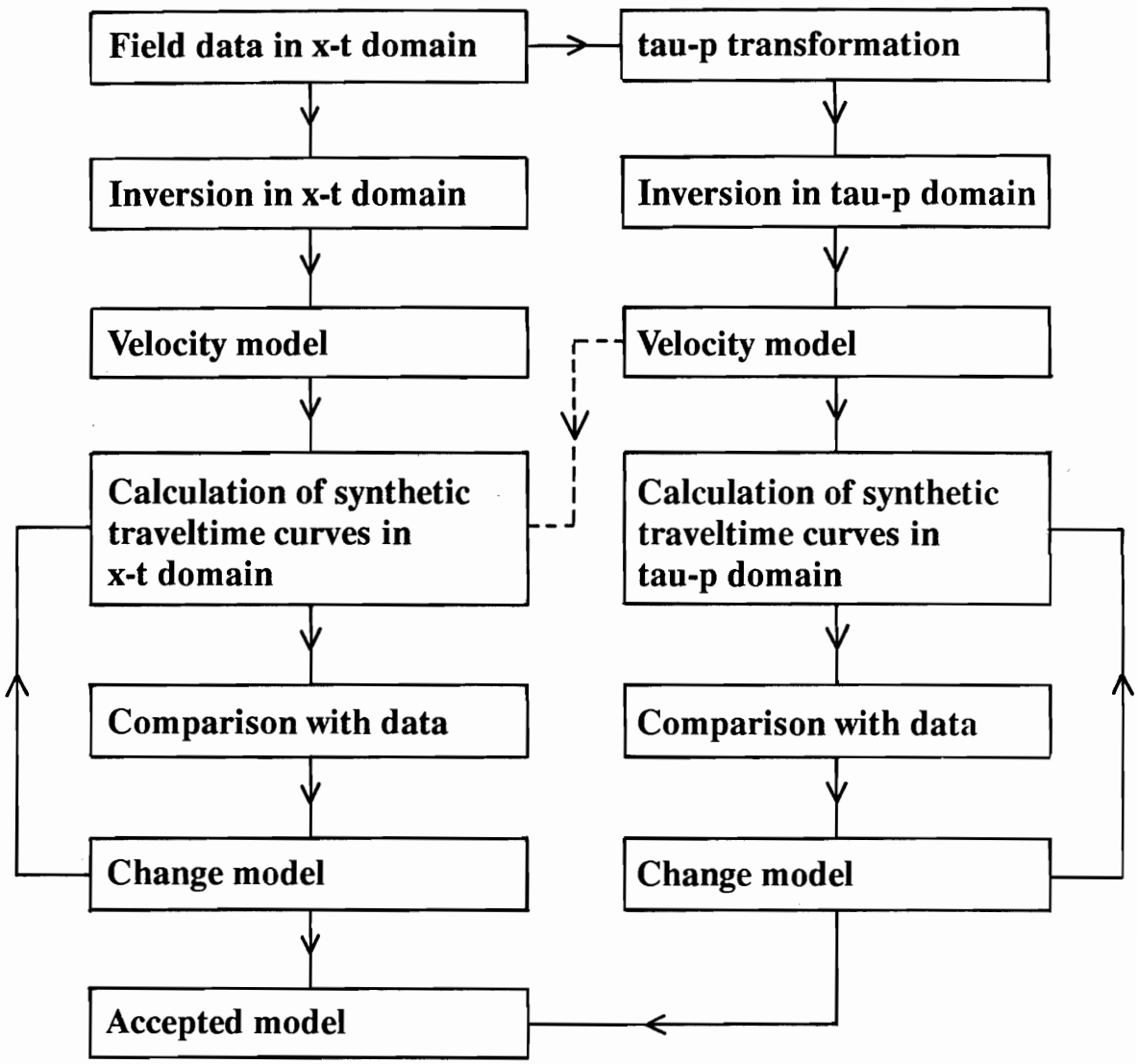

Figure 7

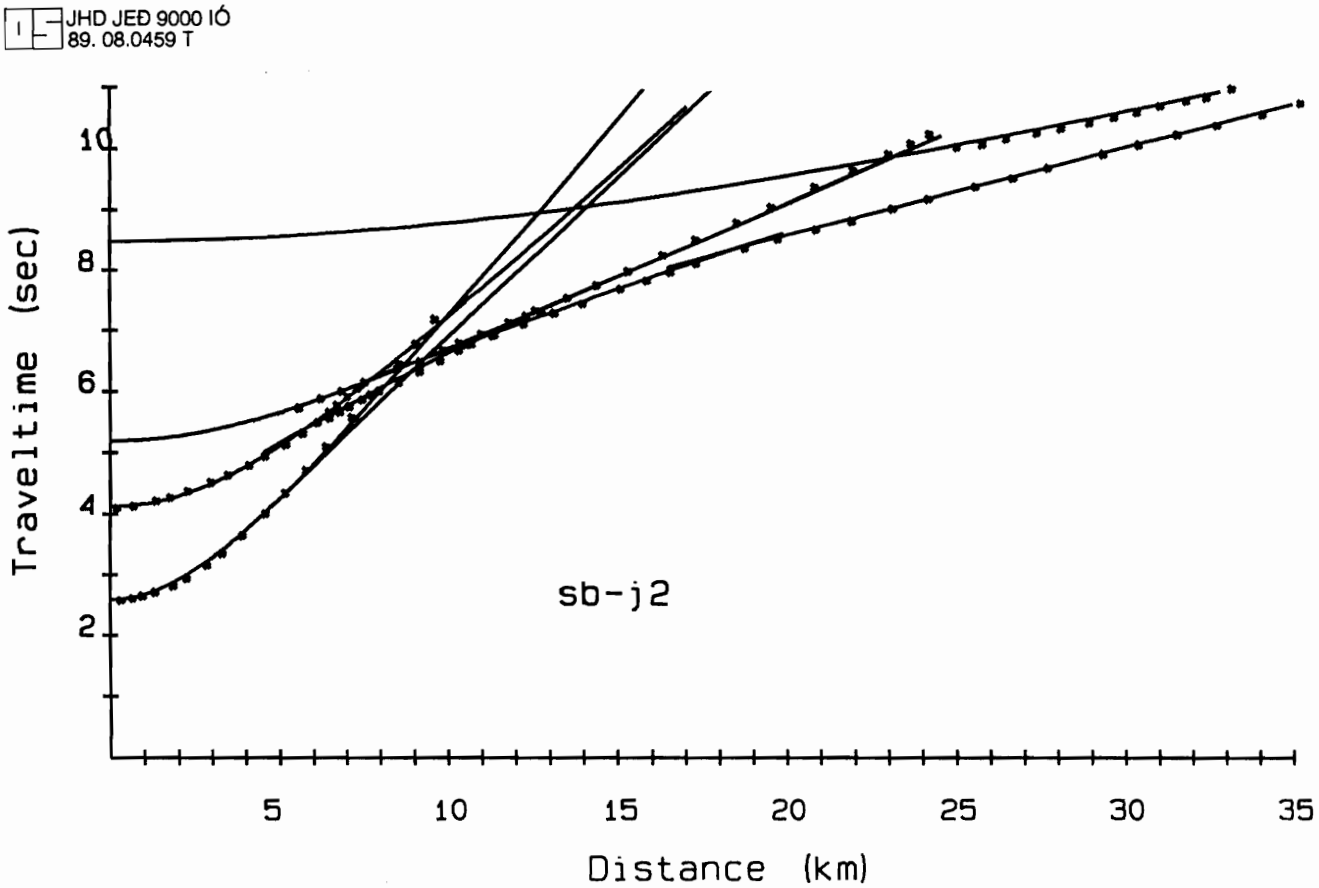
JHD JEÐ 9000 IÓ
89. 08.0459 T
Traveltime (sec)
2
4
6
8
10
sb-j2
5
10
15
20
25
30
35
Distance (km)

Figure 8

JHD JEÐ 9000 IÓ
89. 08.0460 T

Velocity functions for sb 11

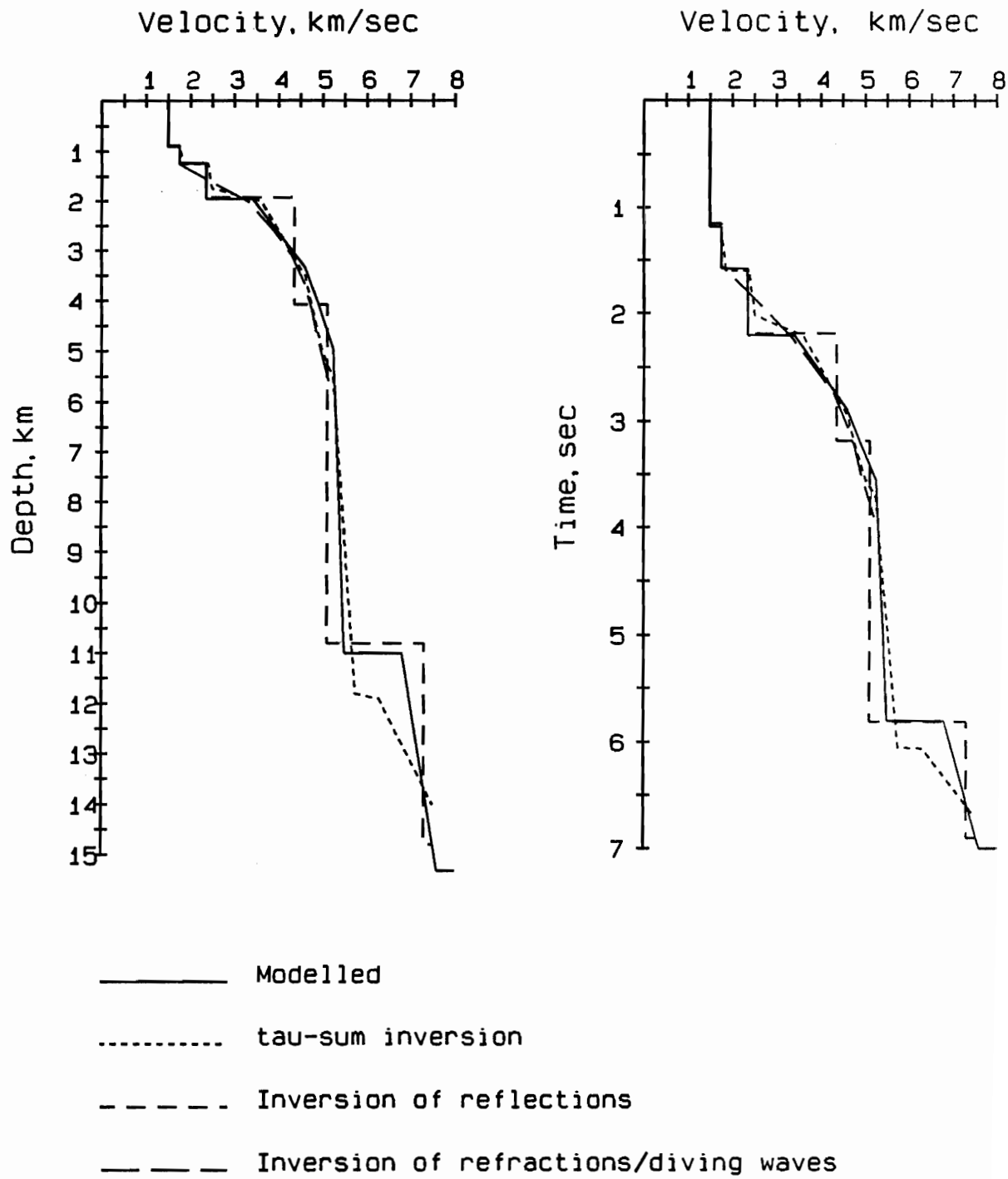

Figure 9

3. Results of the interpretation

The results of the interpretation of the sonobuoy data will be described separately for each of the areas (i), (ii), and (iii). The solutions of the data are also listed in the appendix.

3.1 The east flank of the Jan Mayen Ridge

This area contains the dipping sequence and "normal" oceanic crust of the Norway Basin. The solutions for the sonobuoy profiles in the oceanic crust, east of the dipping sequence, are shown in figure 10. The arrows in the figure point to the reflector JO. The thickness of the sediments above JO varies from about 1.5 km to about 3 km with decreasing thickness to the east and to the north. On profiles 26 and 27 the thickness is 1.2 and 1.3 km, respectively, while, for instance, on profiles 28 and 29 it is about 2.5 km. The velocities in the uppermost 1-1.5 km of the sediments are in all cases in the range 1.7-2.5 km/sec. The deepest part of the sediments above JO, about 1 km thick, has a velocity close to 3.2 km/s. This velocity is not observed above JO on profiles 26 and 27. The velocity structure below JO is typical for oceanic crust, i.e. a strong velocity gradient in layer 2 (ca. 1 s^{-1}) underlain by layer 3 with a very low gradient, close to 0.1 s^{-1} were observed. One notes that the gradient in layer 2 is lower for the sonobuoy profiles shot in the east-west direction (0.8 s^{-1}) than for the profiles shot in the north-south direction (1.18 s^{-1} on average). The thickness of layer 2 is in the range 2-3 km, which is typical for "normal" oceanic crust, except for sonobuoy 26 where the thickness is about 4.5 km. A deep reflection, which we interprete as a reflection from Moho, is observed on sonobuoys 32, 33 and 42. The interpretation of these reflections gives a crustal thickness of 6 to 11 km respectively. In the reflection data, a reflection pattern is observed at about 8 sec twt, which corresponds to the reflection observed on the sonobuoys.

Figure 11 shows the solutions of the sonobuoy profiles shot in the area of the dipping reflector sequence, and also those shot in the area between the main ridge block and the dipping sequence. As mentioned above, some of these profiles are difficult to interpret because of varying dip in layer interfaces. This applies especially to sonobuoys 25 and 18. It is striking that the sedimentary formations above JO can be divided into two main sequences on the basis of the velocity structure. In the upper

one the velocity varies from 1.7-2.0 km/s with an average of 1.9 km/s. The thickness of this sequence is in most cases 1.0-1.5 km. The velocity in the lower sequence varies from 3.1-3.8 km/s, with an average of about 3.4 km/s, and the thickness varies from 1.0 to 3.0 km. On the reflection profiles (NPD/OS report, in preparation) the upper sequence appears as a chaotic reflection pattern while the lower one shows strong reflections, most of which are parallel to the JO horizon.

The velocity structure ovserved below JO depends on the location of the sonobuoy relative to the dipping sequence. The sonobuoy profiles shot along the dipping sequence or those launched in the dipping sequence and shot to the east, all show velocity structure similar to that of the oceanic crust. The velocity just below JO is in most cases 4+ km/s, increasing with depth and reaching 6.7-6.9 km/s at a depth of 2-3 km below basement. Below this level the velocity is fairly constant about, 7 km/s. The thickness of the 7 km/s layer is obtained only in a few cases, and it varies from 5-7 km. The sonobuoys launched in the area to the west of the zone of dipping reflectors show different velocity structure below JO, e.g. J2 and J6. Below JO there is a layer with a low gradient where the velocity increases from 4+ km/s to 5+ km/s (in profile 18 it increases from 4.0 to 4.8 km/s). In sonobuoy profiles 18 and J2 the thickness is 2.0-2.5 km while in J6 it is about 4.3 km. Below this low-gradient layer the velocity structure is similar to that of the profiles located further to the east in the dipping sequence.

3.2 The main ridge block

The thickness of the sediments between JA and JO varies very much in this area, while the thickness above JA is fairly constant, often a few hundred meters. In the area close to the eastern edge of the main ridge block the thickness of the sequence between JA and JO is close to 2 km. In some cases, the thickness of this sequence decreases to nearly zero, especially in the area close to lines JM-11-85 and JM-12-85 (figure 1). This is shown in figure 2. The solutions of the profiles from the area of the main ridge block are shown in figure 12. Sonobuoy profile 44 is located on the western flank of the ridge and will be discussed separately. We did not put much effort into finding the detailed velocity structure in the uppermost sedimentary

sequences, it can better be found from the stacking velocities obtained from the processing of the reflection data. Because the sediments above JA are very thin it was not always possible to find an accurate velocity for this layer, but when possible it was 1.6-1.8 km/s. The velocity structure obtained for the sequence between JA and JO varies, and in some cases is it missing, e.g. sonobuoys 20 and 40. However, on the whole the sequence can be divided into two main units, an upper one in the velocity range 2-2.4 km/s and a lower one in the range 3-3.5 km/s. There is a large jump in the velocity across the horizon JO, except for sonobuoy 11 where a change in the gradient is observed. In most cases the velocity just below JO is 4-4.5 km/s and generally increases slightly with depth. In cases where the depth of observation is great enough, a layer with an average velocity slightly greater than 6 km/s is found at greater depths. The thickness of the sequence between JO and this layer is generally in the range of 2-4 km. The solution for sonobuoy profile 11 does not show the 6+ km/s layer, but the velocity structure in the uppermost 2-3 km below JO is similar to that of the other profiles, e.g. profile 10. About 2 km below the level of JO, on profile 11, the velocity is 5.25 km/s and reaches 5.5 km/s about 8 km below JO, i.e. 11 km below the sea surface. Below this, there is about a 4 km thick layer with an average velocity of 7.2 km/s. A layer with this velocity is also observed on profile 44 (figure 12).

Sonobuoy 44 is located on the west flank of the ridge, shot along line JM-128-85 (figure 1). Reflectors JA and JO are not clearly observed in this region. The reflection data show strong, irregular reflecting segments down to about 6 sec twt at the beginning of the sonobuoy profile (NPD/OS report, in preparation). A strong and continuous reflector is observed at 7.5 sec at the beginning of the profile, but at the end of the profile it is at about 6.5 sec. Below the seafloor there is a 400 m thick layer with a velocity of 1.6 km/s underlain by a 700 m thick layer with a velocity of 2.3 km/s. Below the latter the velocity increases with depth but the gradient decreases, and at a depth of about 9 km below the sea surface the velocity is constant, 6.1 km/s. At greater depths there is a layer with an average velocity of 6.9 km/s. The base of this layer is not well defined, but it seems to be associated with the strong reflection at about 7.5 sec observed in the reflection data, resulting in a 5 km thickness.

Two sonobuoy profiles were shot in the area to the south of the Jan Mayen Trough,

sonobuoys 1 and 2. Sonobuoy profile 1 is shot along a north-south trending rift trough to the west of a basement ridge, while sonobuoy 2 crosses the ridge. The solutions of these profiles are shown in figure 13. The velocity structure in the uppermost 2-3 km below JO is very similar to that of the northern main ridge block. However, on profile 1 at nearly 6 km depth (2.5 km below JO) the velocity increases abruptly from 5.4 km/s to 7.0 km/s, and 2 km deeper there is a possibility of another jump to 7.5 km/s (although we think that this is most likely a single layer). This high velocity layer is similar to the deepest part of profile 11.

3.3 The Jan Mayen Basin

Four sonobuoys are located in the Jan Mayen Basin, and the solutions are shown in figure 14. Two of the profiles reveal a high-velocity layer, about 5 km/s, associated with the opaque layer. We deduce from the weak head waves that this layer is underlain by a layer with a lower velocity. On the two other profiles no refraction associated with the opaque layer is observed. This is probably because of that the opaque layer is too thin to carry a large amount of refracted energy. We do not have information about the velocity of the low-velocity layer, but as it most likely represents Tertiary sediments we have assumed velocity of 2.6 km/s for these formations. This gives a thickness of 1.2 - 2.0 km for this layer. Below the low-velocity, layer a refractor is observed, giving a velocity of 4.7 - 4.8 km/s, except for the westernmost sonobuoy, sb-38, where the velocity is about 5.4 km/s. The larger offsets of sonobuoy profile 43 are recorded outside the limit of the opaque layer at the western extension of the ridge proper (see figure 1). For the shot points in this area, deeper refracted arrivals are observed, giving the average velocity of 6.15 km/s. The thickness of this layer is uncertain, but it is probably close to 4 km.

3.4 Velocity cross sections across the ridge

Cross sections showing isovelocity curves have been drawn for 4 seismic lines, i.e. JM-2, JM-8, JM-11, and JM-14. Sonobuoys on or close to these lines have been used. The cross sections are shown in figures 15, 16, 17, and 18. The sonobuoys used and the depth to horizon JO are indicated. The depth to what we think is Moho is marked

by M. This curve is not an isovelocity curve; it is rather the deepest part observed, mapped by wide angle reflections. The location of the zone of the wedges of dipping reflectors is shown in the figures (WDR). It is striking that the reflector JO follows closely the isovelocity curve 4 km/s, except at the western half of the ridge block, where it is between the 2 and 3 km/s isolines.

In the easternmost part of the sections, the velocity structure below JO is typical for oceanic crust, i.e. a strong velocity gradient in the uppermost part and a nearly constant velocity in the lower part. The oceanic crustal thickness is not clearly observed except on line JM-11 (figure 17), where the thickness increases when approaching the dipping sequence. It is the deeper part whose thickness increases, while the gradient layer (layer 2) seems to be fairly constant in thickness.

It is striking how the thickness of the sequence between the 5 and 6 km/s isolines increases below the eastern part of the ridge. This thick zone is located to the west of, and partly below, the dipping sequence. This is not clearly observed on the northernmost line, line JM-2. One also notes that the thickness of the sediments between the seafloor and horizon JO reaches a maximum at the eastern end of this zone.

It is only on line JM-11 that we have data from the Jan Mayen Basin area to the west of the main ridge block (figure 17). It is clear that isovelocity curves of 3 km/s and higher extend to underneath the opaque layer in the basin. The opaque layer is shown as a heavy black streak in figure 17.

The depth to Moho below the ridge block varies from 13 to 15 km and decreases slightly below the Jan Mayen Basin (figure 17). In the oceanic crust, the Moho depth is 14-17 km, resulting in a 6-10 km thick oceanic crust.

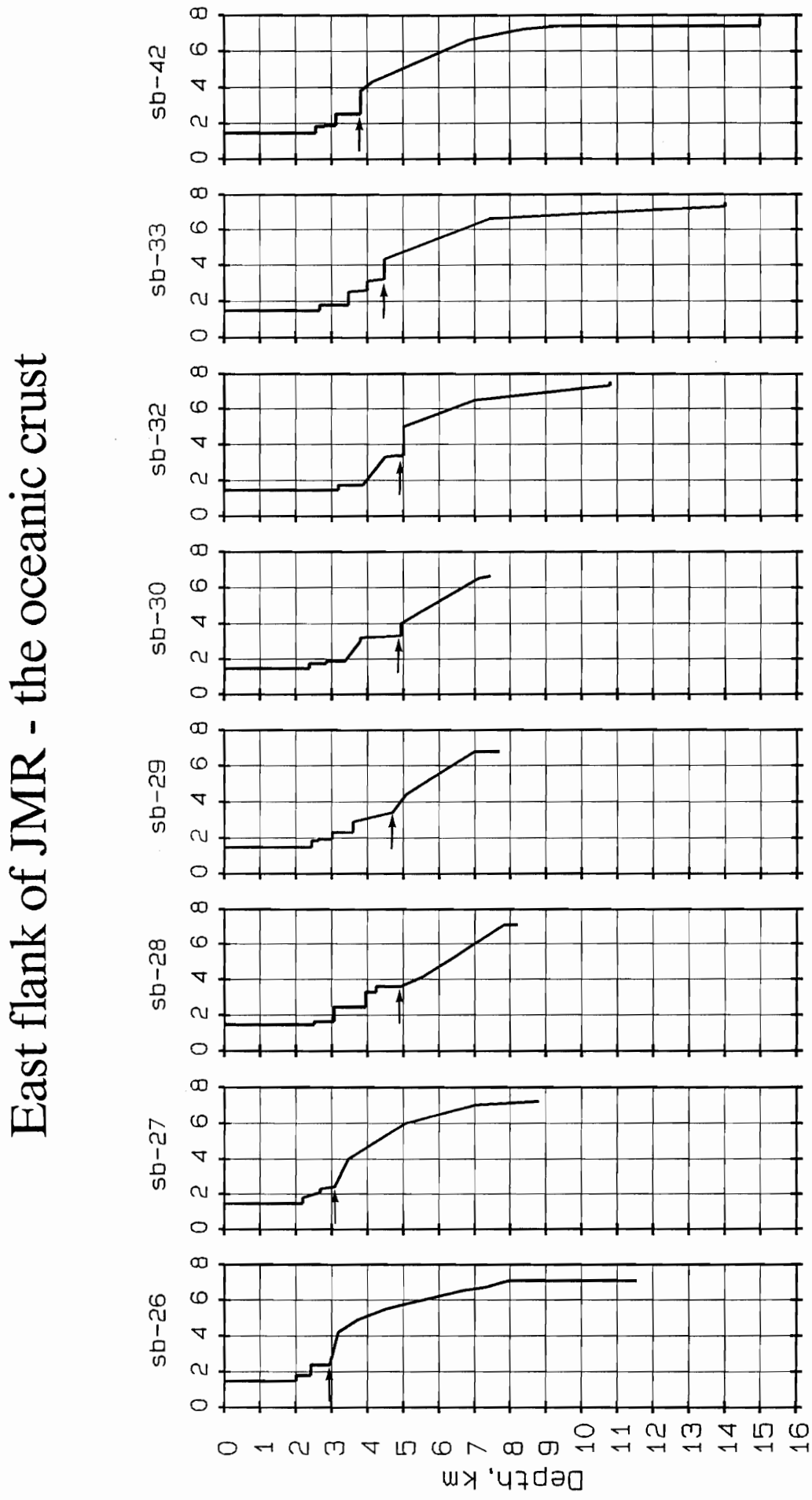
East flank of JMR - the oceanic crust
sb-42
sb-33
sb-32
sb-30
sb-29
sb-28
sb-27
sb-26
0 2 4 6 8
0 1 2 3 4 5 6 7 8 9 10 11 12 13 14 15 16
Depth, km
JHD JEÐ 9000 IÓ
89. 08.0461 T

Figure 10

East flank of JMR - the area of the dipping sequence

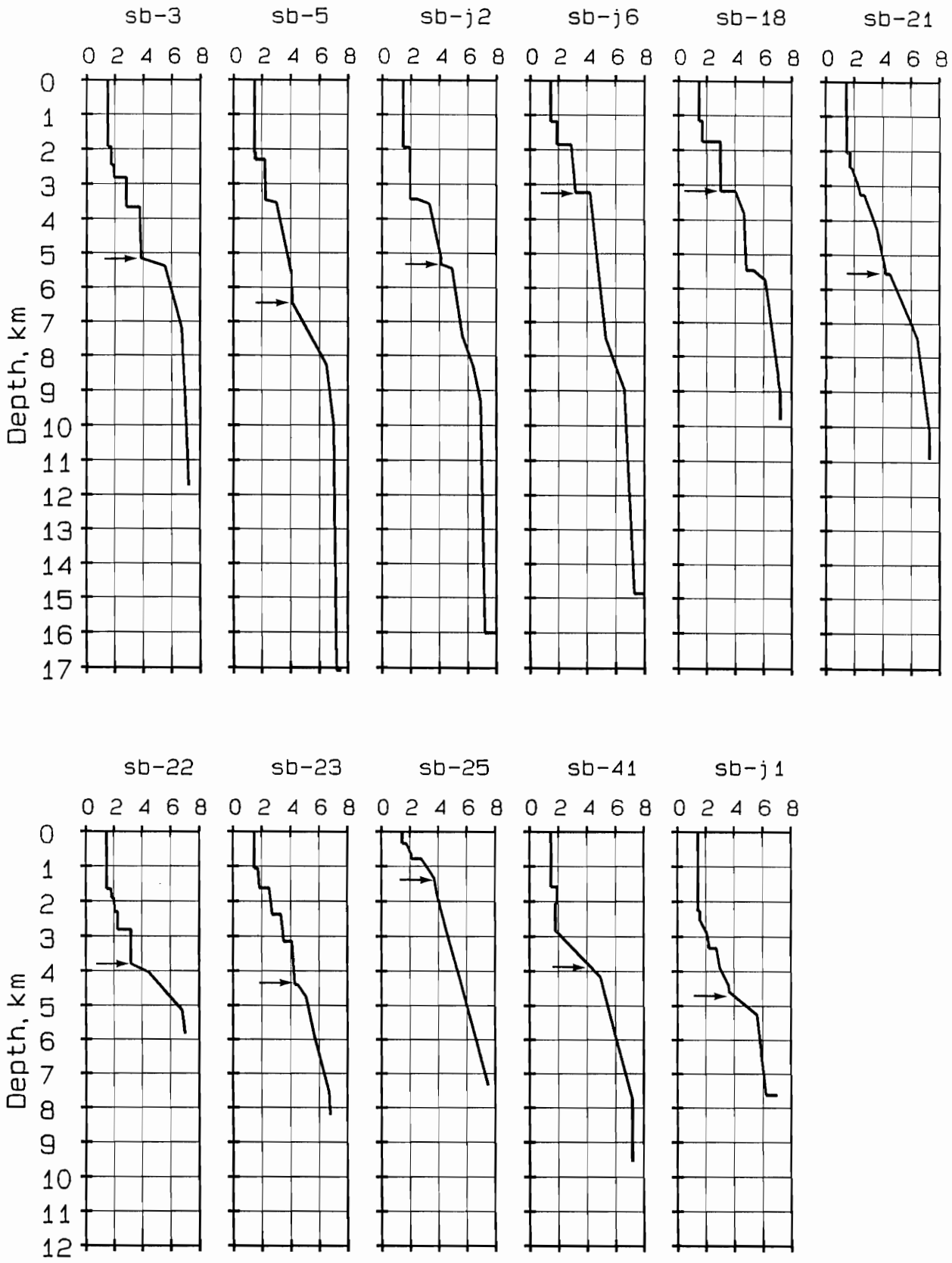

Figure 11

JHD JEÐ 9000 IÓ
89. 08.0462 T

The main ridge block of the northern JMR

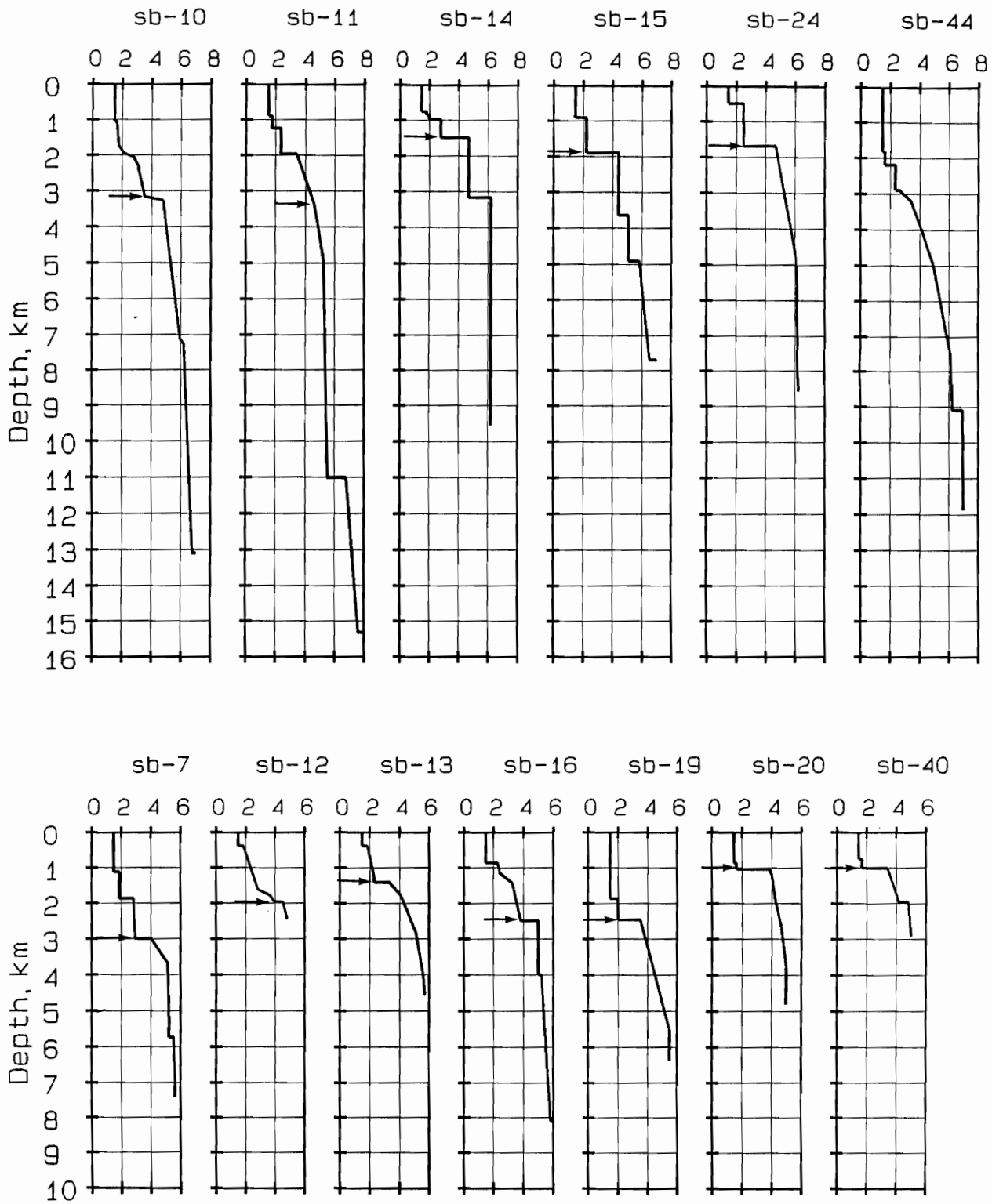

Figure 12

JHD JEÐ 9000 IÓ
89. 08.0463 T

Southern part of JMR

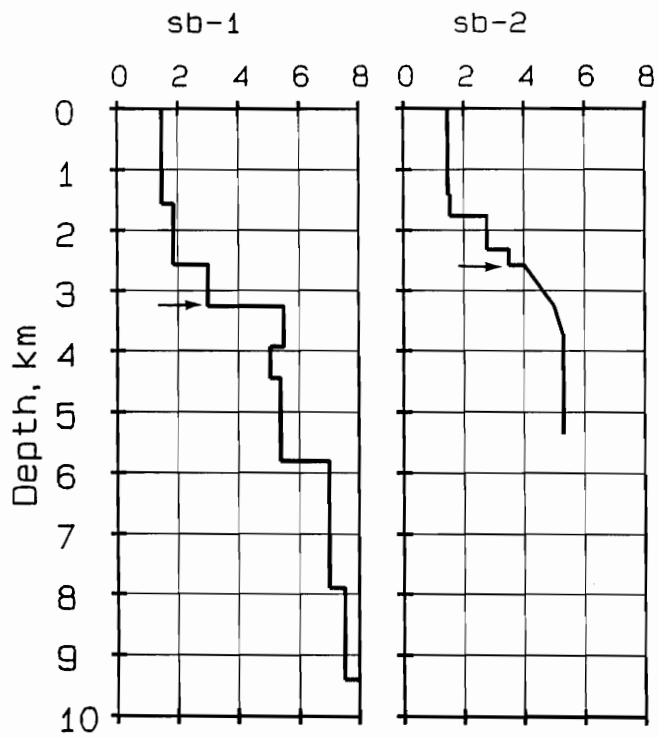

Figure 13

Jan Mayen Basin

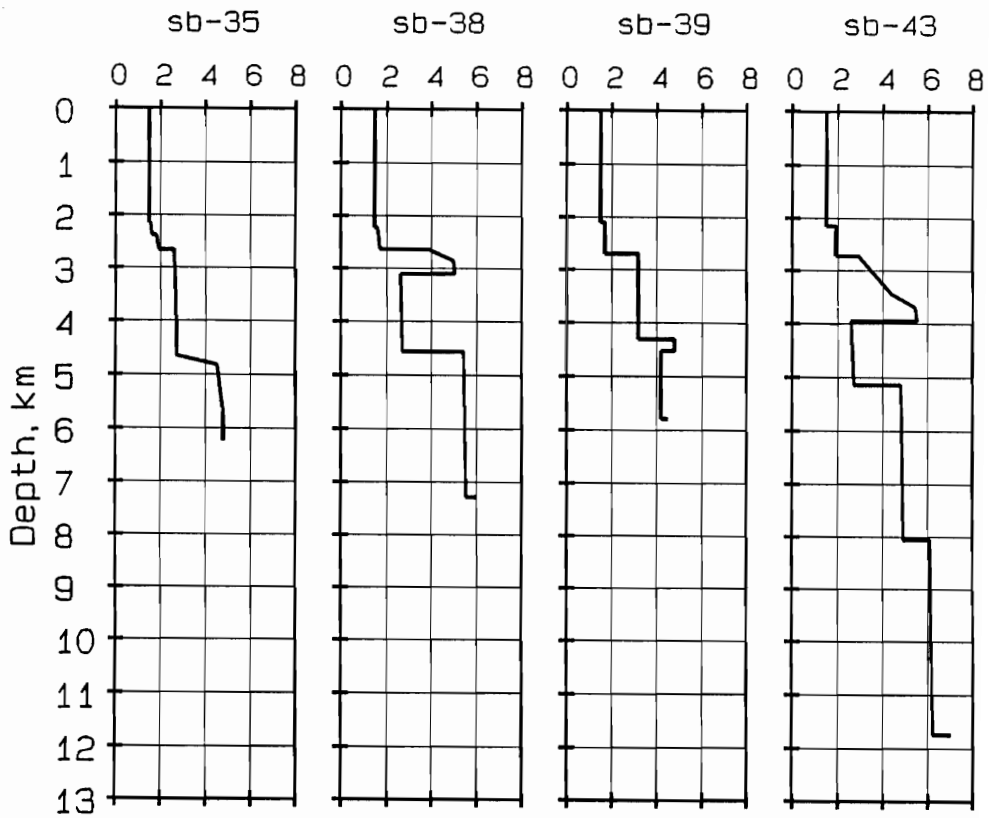

Figure 14

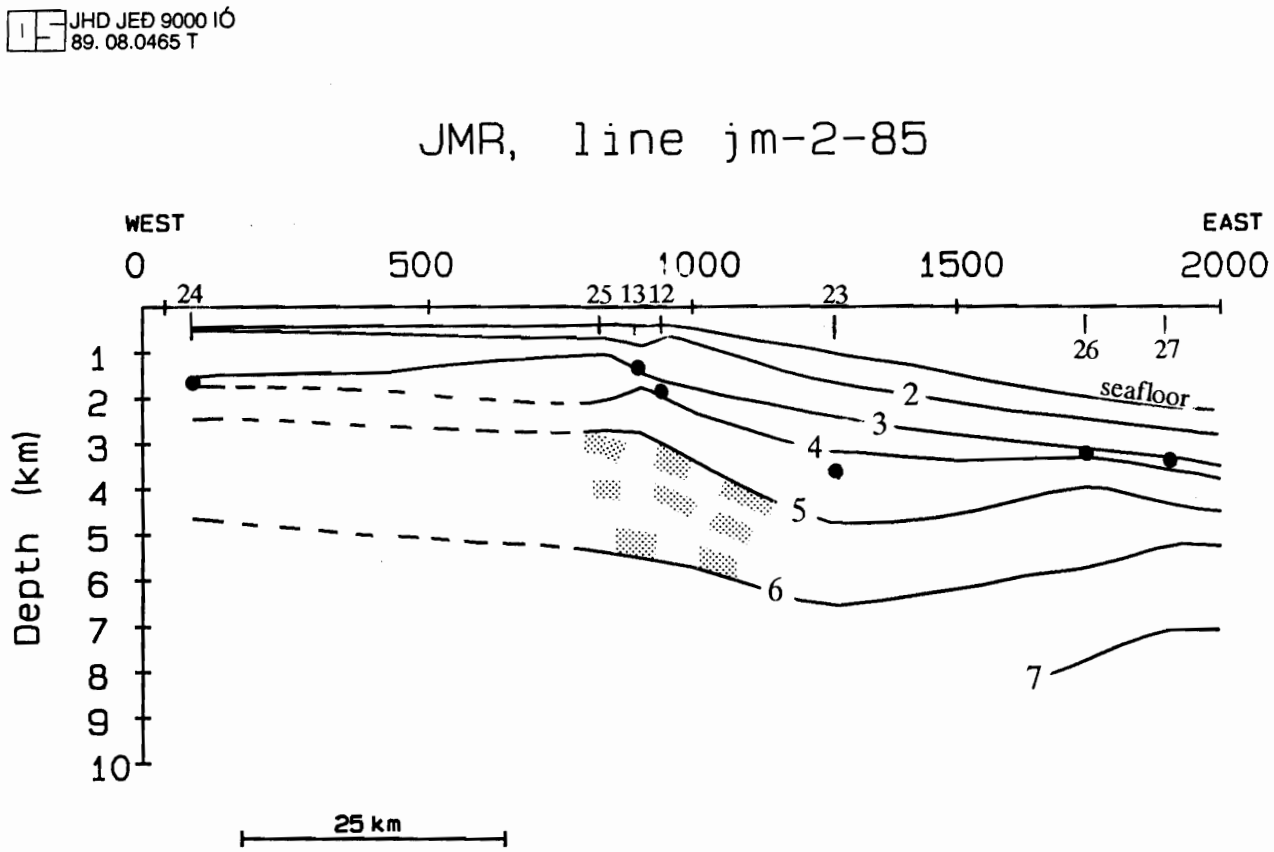
JHD JEÐ 9000 IÓ
89. 08.0465 T
JMR, line jm-2-85
WEST
EAST
0
500
1000
1500
2000
24
25 13 12
23
26
27
seafloor
2
3
4
5
6
7
Depth (km)
1
2
3
4
5
6
7
8
9
10
25 km

Figure 15

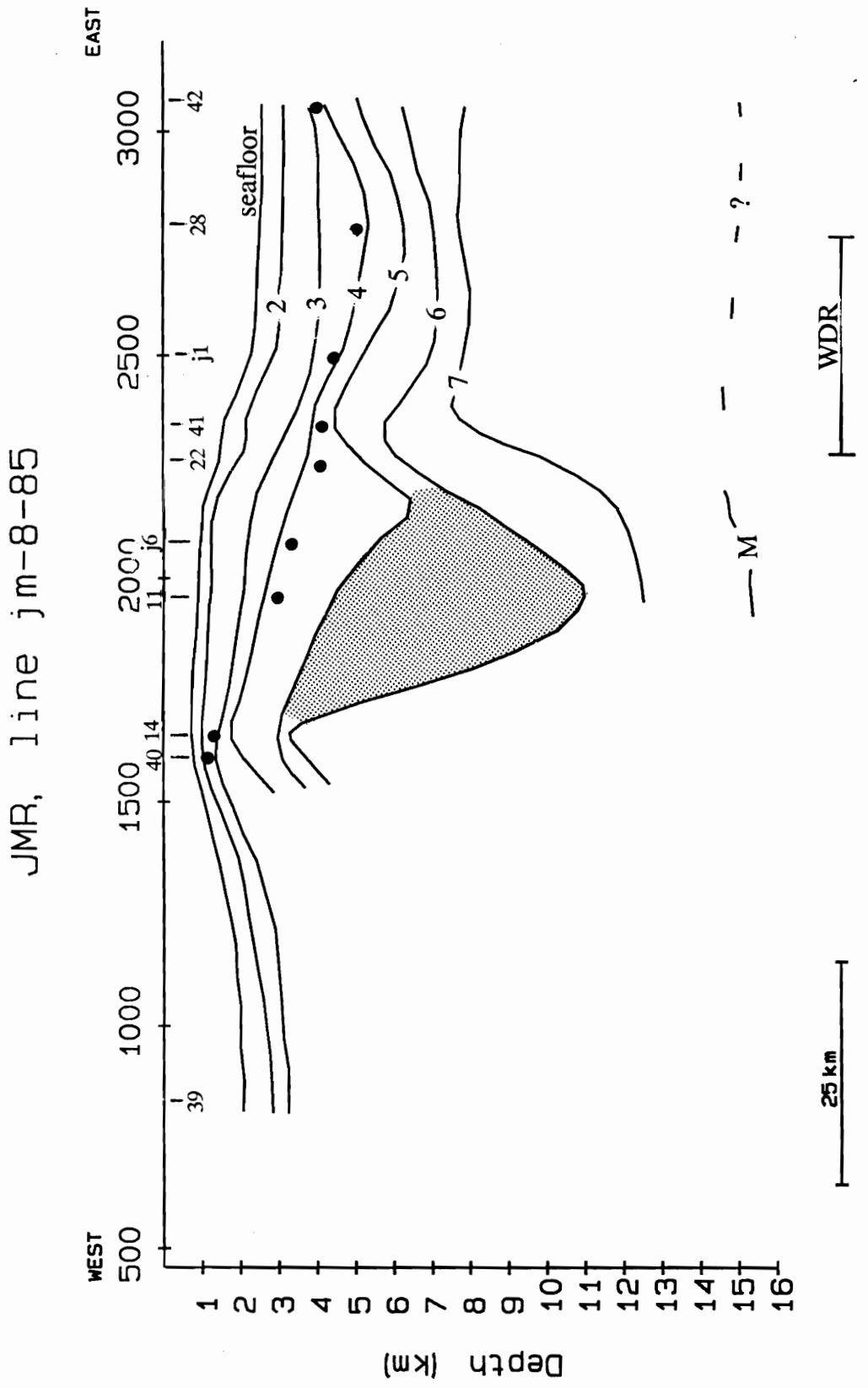
JMR, line jm-8-85
WEST
EAST
500
1000
1500
2000
2500
3000
seafloor
2
3
4
5
6
7
M
WDR
25 km
Depth (km)
1
2
3
4
5
6
7
8
9
10
11
12
13
14
15
16

Figure 16

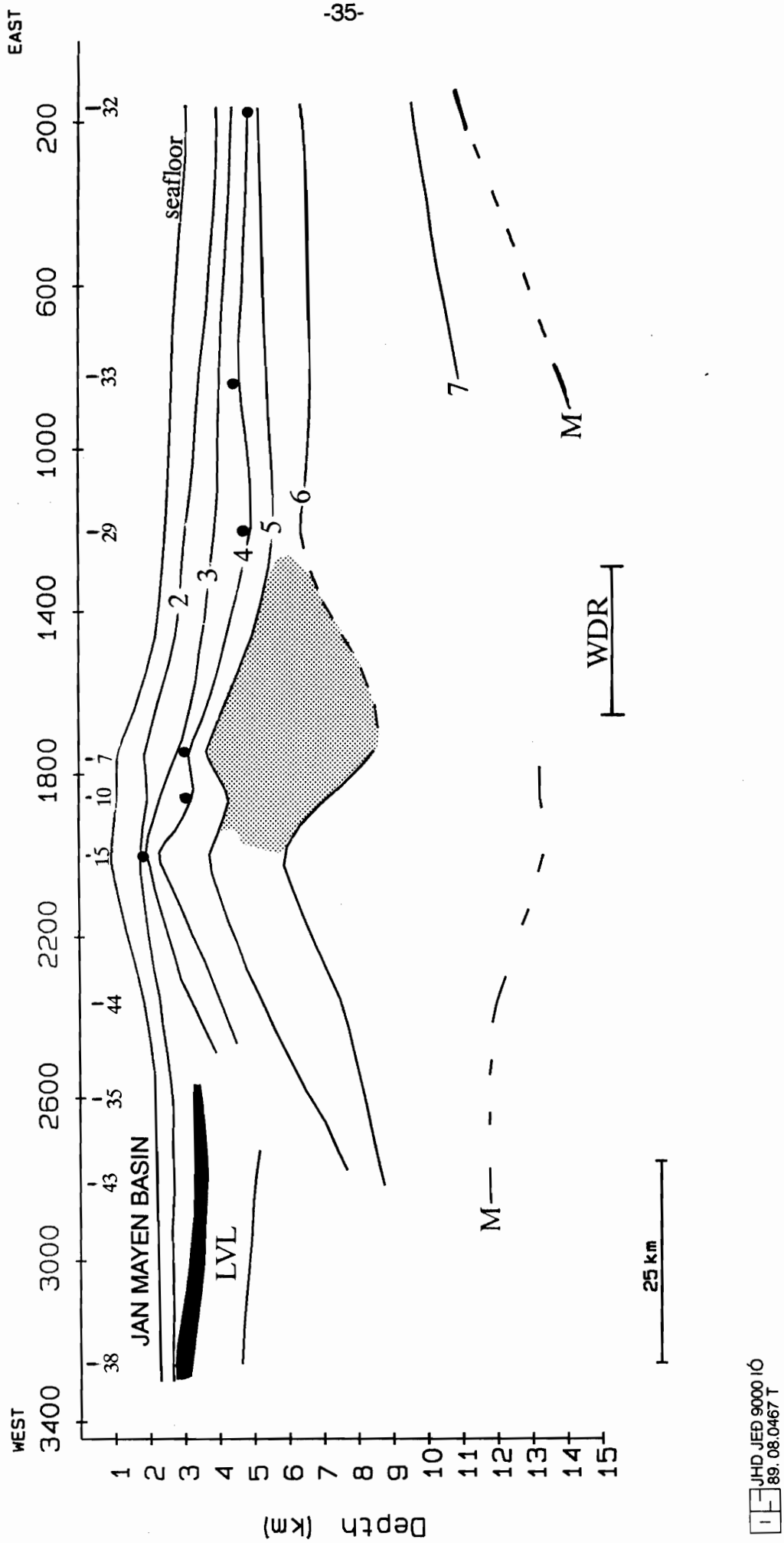
JMR, line jm-11-85
WEST
EAST
3400
3000
2600
2200
1800
1400
1000
600
200
38
43
35
44
15
10
7
29
33
32
seafloor
2
3
4
5
6
7
JAN MAYEN BASIN
LVL
M
M
WDR
25 km
Depth (km)
1
2
3
4
5
6
7
8
9
10
11
12
13
14
15
JHD JED 9000 IÓ
89. 08.0467 T

Figure 17

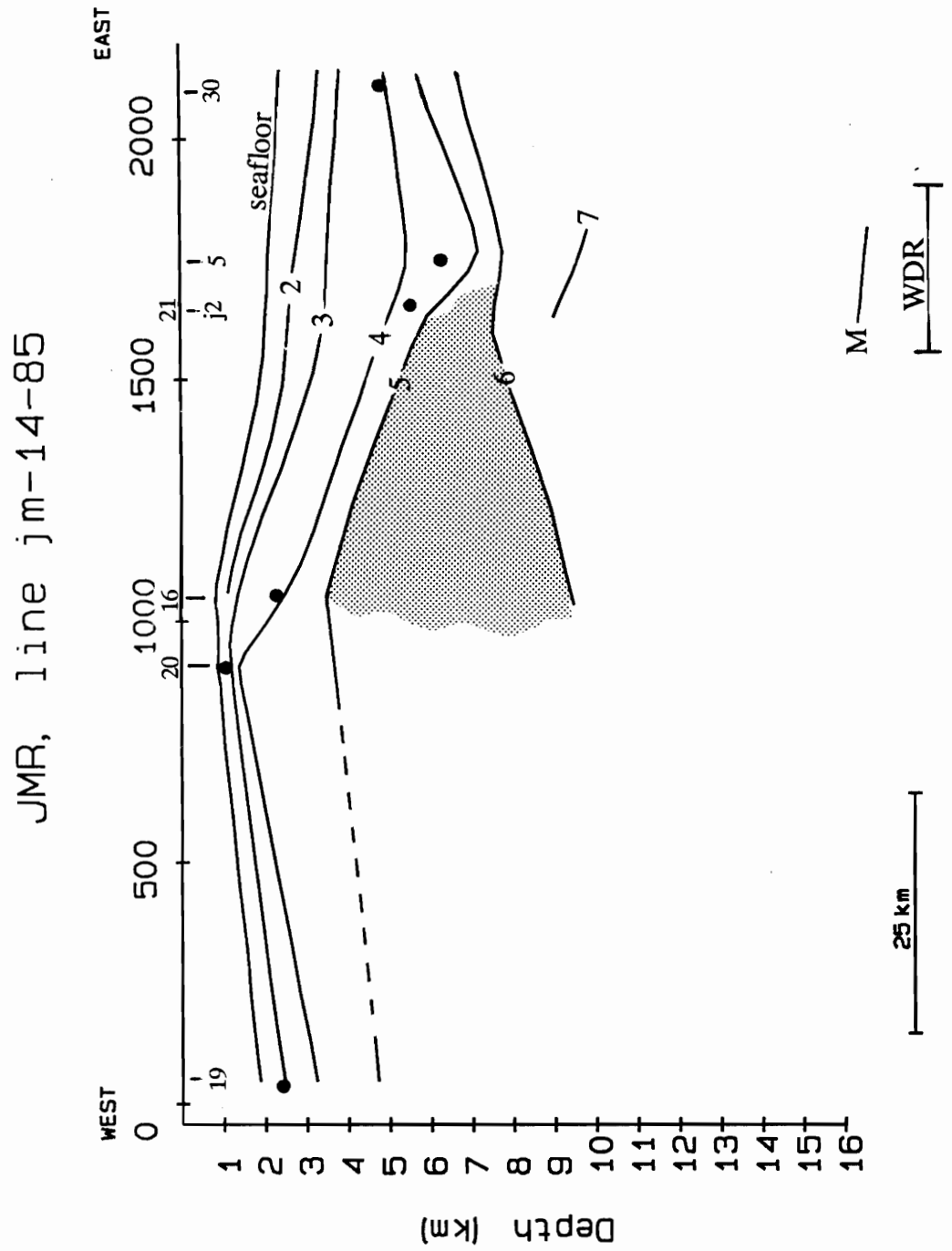
JMR, line jm-14-85
WEST
EAST
0
500
1000
1500
2000
19
20
16
21
j2
5
30
seafloor
2
3
4
5
6
7
M
WDR
25 km
Depth (km)
1
2
3
4
5
6
7
8
9
10
11
12
13
14
15
16
JHD JED 9000 IÓ
89. 08.0468 T

Figure 18

4. Discussion and summary

4.1 Discussion

Seismic velocity itself is not a simple indicator of crustal type, i.e. oceanic, continental, or sedimentary. However, if one looks at the velocity structure of the entire crust, then there is a characteristic difference between oceanic and continental basement. Also, the sedimentary velocities are usually much lower than the oceanic and the continental basement velocities, although old compact sediments can have velocities comparable to the basement velocities. Identification of different sedimentary sequences from the knowledge of the velocity-depth structure can be speculative. However, a comparison of velocity-depth functions on the Norwegian margin with reflection profiles where the age of different formations is known shows a definite pattern (Eldholm and Mutter, 1986; Ólafsson, 1988). The results of two ESP profiles from the Møre Basin are shown in figure 19 (Ólafsson, 1988). The Tertiary sequence can usually be divided into 2-3 main layers on the basis of different velocities. Usually the velocity reaches about 2.6 km/s at the base of the Tertiary sequence. The maximum thickness of the underlying Cretaceous sediments is more than 5 km. In the uppermost 1-1.5 km the velocity increases from 2.9 to 3.7 km/s, while in the lower part the gradient is very small. At the base of the Cretaceous sequence the velocity generally reaches about 4.2 km/s. Below the Cretaceous sequence the velocity increases abruptly from 4.2 to about 5 km/s. At greater depth, a sudden velocity increase from less than 6 km/s to 6+ km/s is observed on many profiles. This velocity increase has been interpreted as representing the transition from sediments to continental basement (Eldholm and Mutter, 1986).

The results of the velocity analysis from the Jan Mayen Ridge area show that the Tertiary sedimentary sequence, i.e. the sediments above JO, can be divided into two main units. The velocity in the upper one is in the range of 1.7-2.5 km/s, but in the range of 3-3.5 km/s in the lower one. The velocity structure in the upper unit is very similar to that of the Tertiary sequence on the Norwegian margin, while the lower one has much higher velocities. The lower unit seems to represent sediments deposited on the Jan Mayen Ridge in the Early Tertiary, which are not present on the Norwegian margin. Therefore, these sediments are most likely from Greenland and were

deposited on the ridge while it was a part of the continental margin of East Greenland after the breakup of Norway and Greenland.

The velocity structure of the formations below JO depends on the location, i.e. whether they are in the main ridge block or in the area of the dipping sequence and further east. Figure 20 shows the difference between these two areas. All the solutions were adjusted such that the depth to JO was the same. It is striking that the velocities in the east flank of the ridge are higher than those below the main block. The velocity structure in the east flank is typical for oceanic crust, i.e. high velocity gradient in the uppermost part, but much lower in the lower part. This is seen in figure 21 where two ESP profiles (elf-45 and elf-46 from Ólafsson, 1988) from oceanic crust of anomaly 24 time off the Møre margin are compared with the east flank of the Jan Mayen Ridge. The crustal thickness in the area of the dipping sequence on the ridge is not extremely large as it is on the Norwegian margin.

The velocities below JO on the main ridge block are much lower than those of the oceanic crust. If one compares the velocities in the Møre Basin with those below JO on the main ridge block, then one notes that the velocity structure below Base Cretaceous in the Møre Basin fits very well with the Jan Mayen Ridge. Figure 22 shows the solutions of two ESP profiles (elf-38 and elf-40 from Ólafsson, 1988) from the Møre Basin together with the solutions from the Jan Mayen Ridge, where the Base Cretaceous level of the Møre Basin is adjusted so that it coincides with JO. It is not possible to find velocity functions on the Jan Mayen Ridge that are comparable with the Cretaceous sequence on the Norwegian margin. Therefore, we suggest that thick layers of Cretaceous sediments are not to be found on the Jan Mayen Ridge. Cretaceous sediments can of, course, exist as thin layers or in some local areas, but not as a prominent part of the sedimentary sequence as on the Norwegian margin.

A dominating feature of the formations below the horizon JO is the great thickness of the 5-6 km/s sequence (figures 16, 17, 18, and 23). Figure 23a displays a line drawing of reflection profile JM-11, and figure 23b shows isovelocity lines where the depth is given as two-way traveltime. One notes that the 5-6 km/s pocket is associated with the area to the west of, and partly below, the dipping sequence. The area of maximum thickness of the 5-6 km/s pocket is, in all cases, located to the west of the dipping

sequence (figures 16, 17, 18, and 23). The nature and origin of this layer are not clear. The reflection data show clear parallel reflections below JO in this area. To judge from the velocities, these reflectors could be of similar origin as the dipping sequence, i.e. basalt flows or old pre-Cretaceous sediments. It is also possible that this is the uppermost part of some sort of a contaminated continental crust. The transition between sediments and crystalline continental basement is not easily observed. Eldholm and Mutter (1986) argue that on the Norwegian margin the continental basement is associated with changes in velocity gradient and that the velocity of 6+ km/s represents basement. There are only a few sonobuoys on the main ridge block where similar velocity structures are observed, i.e. sb-10, sb-14, sb-15, sb-24, sb-44, and sb-43. All these sonobuoys are located to the west of the 5-6 km/s pocket. From these sonobuoys and comparison with the Norwegian margin, it is reasonable to assume the continental basement, at least below the western half of the ridge, to be represented by the 6+ km/s. This implies very thin crust in the basin to the west of the ridge (figure 17) and that up to 5 km of sediments are to be found below the opaque layer in the basin.

The structures observed below the Jan Mayen Ridge area are similar to those observed on the Outer Møre margin. Figure 24 shows a velocity cross section of the Jan Mayen Ridge and the Outer Møre margin (the results from the Møre margin are from Ólafsson, 1988). Many of the same structures are seen on both margins, although it seems that many of them are larger on the Møre margin than on its counterpart, the Jan Mayen Ridge. The dipping reflector sequence is larger and better observed on the Møre margin; the thickness of the oceanic crust in the area close to the dipping sequence is thicker on the Norwegian side, and a landward facing escarpment (FSE) is clearly observed on the Norwegian margin, but has no counterpart on the Jan Mayen Ridge. Also, the thickness of the 5-6 km/s layer is greater on the Norwegian margin than on the Jan Mayen Ridge. Several explanation of this asymmetry are possible. If the spreading center is located in a transitional environment with an ocean to the east and the "highlands" of Greenland to the west, then one would expect most of the lava produced to flow to the east. When the lava reaches the sea water it cools, and over time an escarpment will have formed by the build-up of flood basalts. Smythe et al. (1983) also proposed this origin of the Faeroe-Shetland Escarpment. The reason for the asymmetry in the oceanic crustal

thickness could be associated with asymmetrical seafloor spreading or a small westward jump of the spreading axis before anomaly 24 time.

The nature and origin of the Norwegian continental margin have been extensively studied by many authors, and many models of the geodynamic mechanisms have been proposed. When discussing the nature and origin of different sequences in the area of the dipping reflector sequence, i.e. close to the ocean-continent transition, one must keep in mind that the geodynamic processes could be responsible for some of these velocity structures, e.g. the 5-6 km/s pocket to the west of the dipping sequence. We will not discuss this further here but point to some excellent recent reports describing the passive margins of the Norwegian-Greenland Sea, i.e. Eldholm et al. (1989), Skogseid and Eldholm (1989), Hinz et al. (1987), Mutter et al. (1988).

4.2 Summary

The Tertiary sequence of the Jan Mayen Ridge, i.e. the sequence between the seafloor and horizon JO, can be divided into two main units. The upper one has a velocity distribution comparable to the Tertiary sequence on the Norwegian margin. The lower sequence, on the other hand, has higher velocities, i.e. 3.0-3.7 km/s. This is interpreted as Early Tertiary sediments originating from Greenland. Tertiary sediments in this velocity range are not observed on the Norwegian margin.

On the basis of the velocity structure below JO, the study area can be divided in two: the main ridge block, and the area of the dipping sequence and the area further east. In the area of the dipping sequence the velocity structure below JO is typical for oceanic crust. The crust is not of extreme thickness in the area of the dipping sequence as is the case on the Norwegian margin. The velocity structure below JO on the main ridge block is best explained as pre-Cretaceous sediments underlain by continental basement rocks. Velocity structures typical of Cretaceous sediments are not observed on the ridge. It is striking that to the west of the dipping sequence, and partly below it, the thickness of the 5-6 km/s sequence increases abruptly. This layer could represent pre-Cretaceous sediments, or it could possibly be associated with some anomalous crust formed in the starting phase of seafloor spreading in the early

Tertiary.

In the Jan Mayen Basin, west of the ridge, a shallow high-velocity basaltic layer ("the opaque layer") is underlain by sediments, up to 5 km thick.

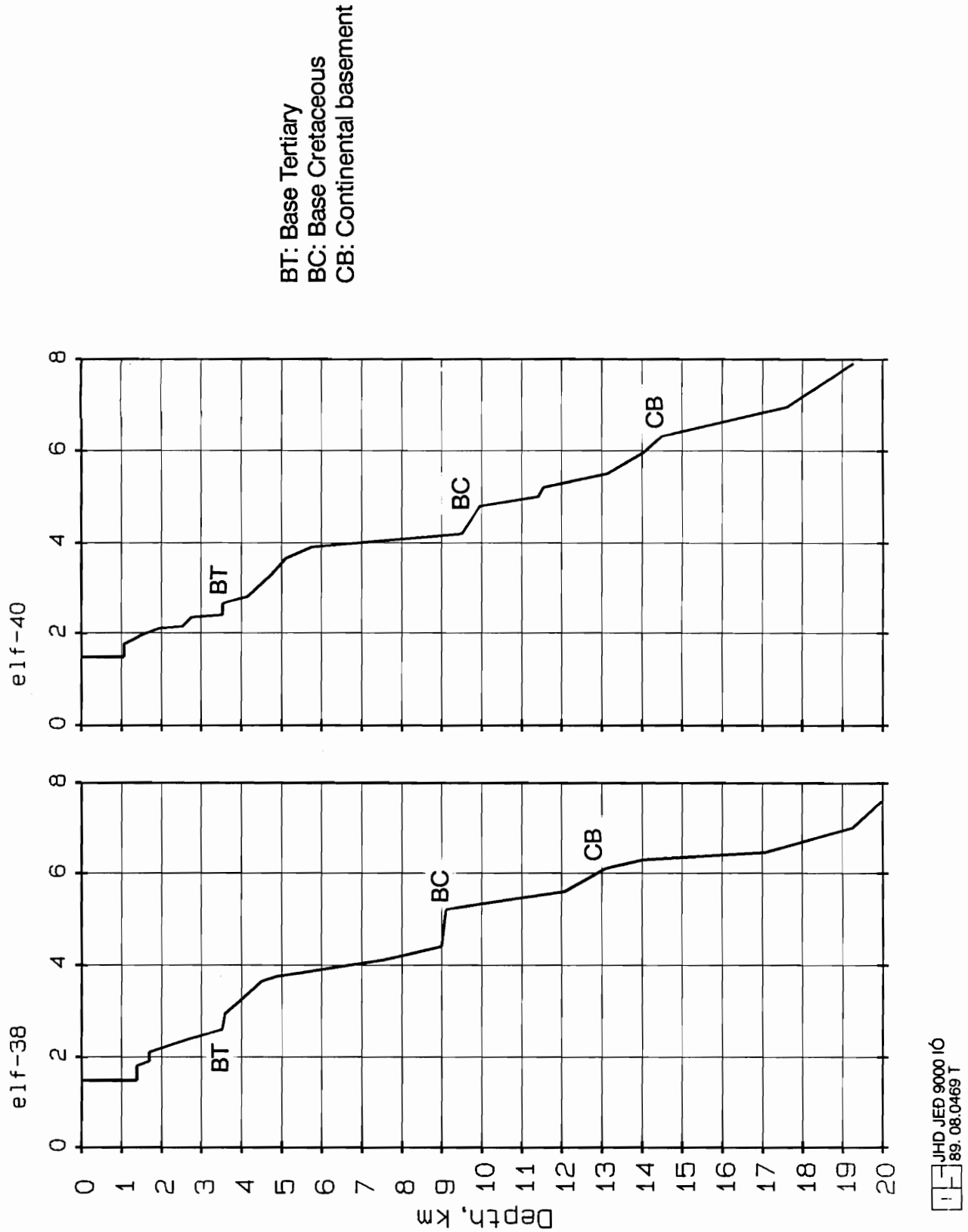
Norwegian Margin
Møre Basin
BT: Base Tertiary
BC: Base Cretaceous
CB: Continental basement
elf-38
elf-40
BT
BC
CB
Depth, km
0 1 2 3 4 5 6 7 8 9 10 11 12 13 14 15 16 17 18 19 20
0 2 4 6 8
JHD JED 9000 IÓ
89. 08.0469 T

Figure 19

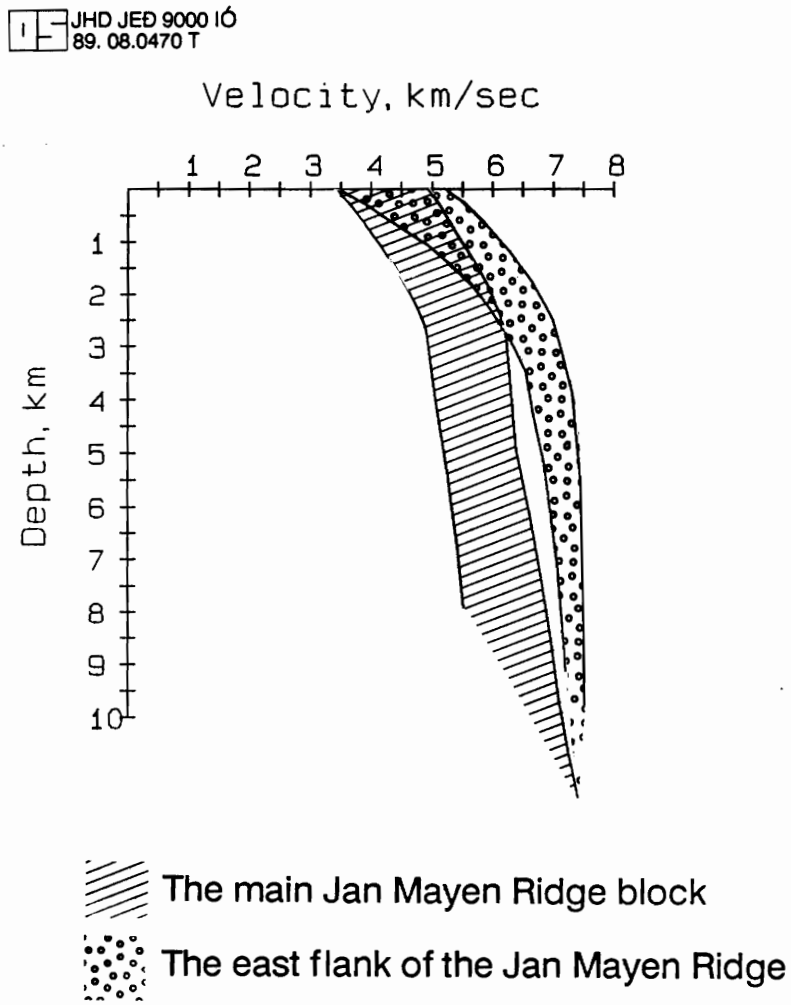
JHD JEÐ 9000 IÓ
89. 08.0470 T
Velocity, km/sec
1 2 3 4 5 6 7 8
Depth, km
1 2 3 4 5 6 7 8 9 10
The main Jan Mayen Ridge block
The east flank of the Jan Mayen Ridge

Figure 20

JHD JEÐ 9000 IÓ
89. 08.0471 T

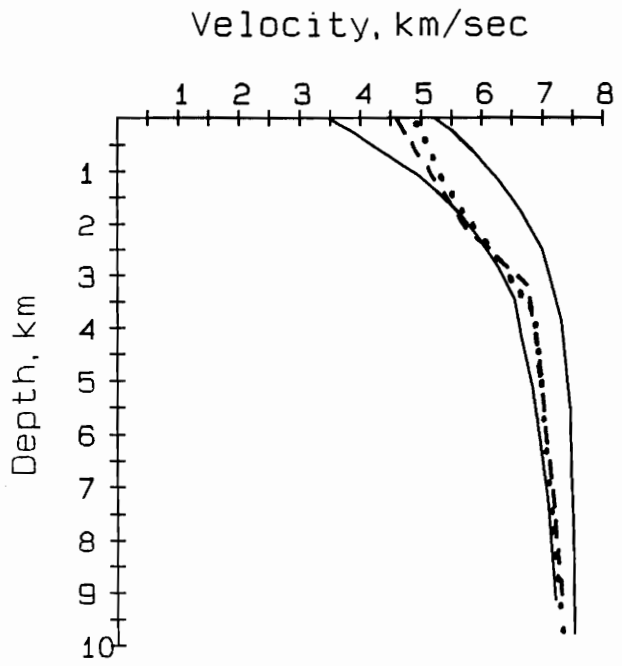

Figure 21

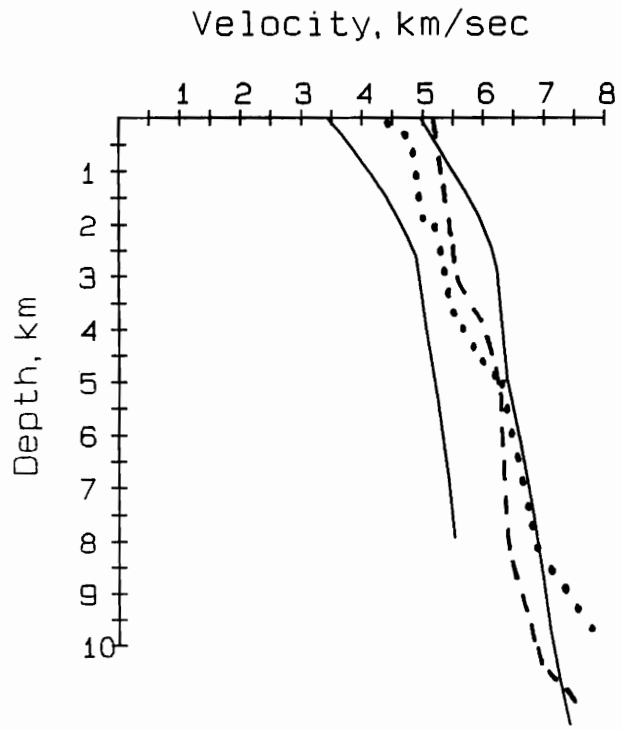

Figure 22

JMR, line jm-11-85

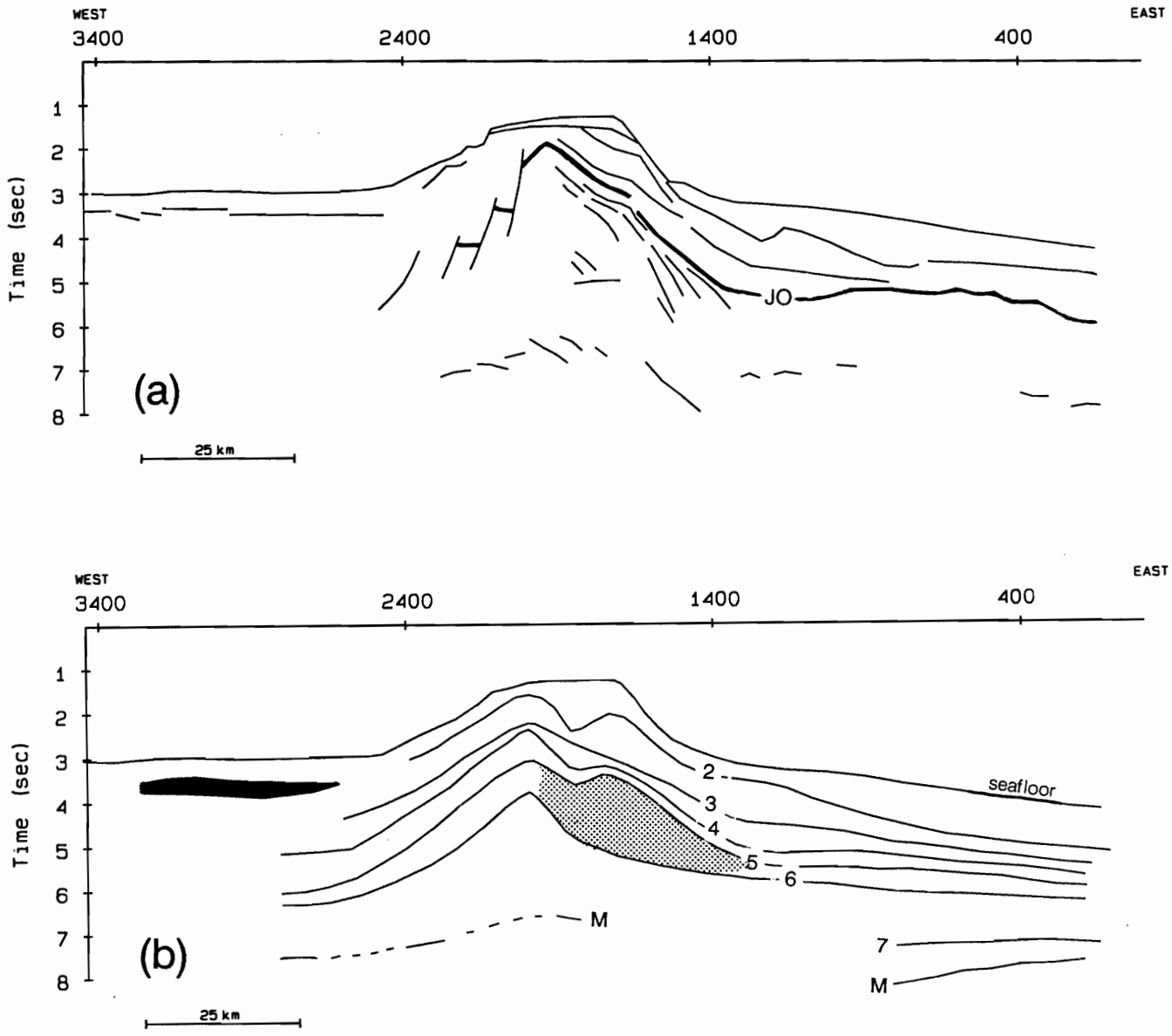

Figure 23

JHD JEÐ 9000 IÓ
89. 08.0472 T

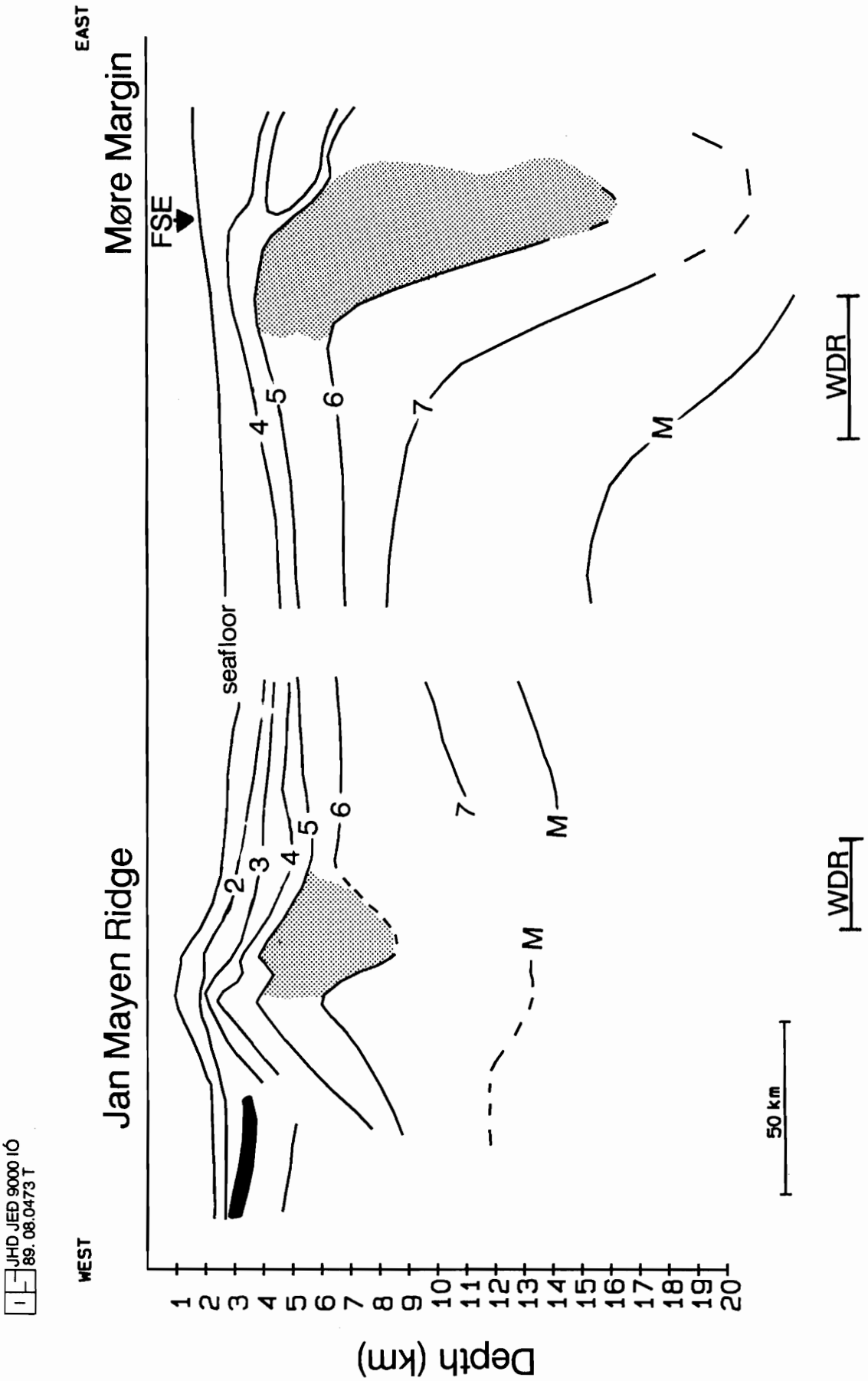
WEST
EAST
Jan Mayen Ridge
Møre Margin
FSE
seafloor
2
3
4
5
6
7
M
WDR
WDR
50 km
Depth (km)
1
2
3
4
5
6
7
8
9
10
11
12
13
14
15
16
17
18
19
20
JHD JED 9000 16
89. 08.0473 T

Figure 24

References.

Diebold, J. B. and Stoffa, P. L. 1981. The traveltime equation, tau-p mapping and investigation of common midpoint data. Geophysics, 46, 238-254.

Eldholm, O. and Mutter, J.C. 1986. Basin structure on the Norwegian margin from analysis of digitally recorded sonobuoys. J. Geophys. Res., 91, 3763-3783.

Eldholm, O., Thiede, J., Taylor, E. et al. 1987. Summary and preliminary conclusions, ODP Leg 104, in Proc., Init. Repts. (pt. A.), ODP, 104, 751-771.

Eldholm, O., Thiede, J and Taylor, E. 1989. Evolution of the Vøring volcanic margin. Submitted to Proc. Scientific Results ODP 104.

Gairaud, H., Jacquart, G., Aubertin, F. and Beuzart, P. 1978. The Jan Mayen Ridge, synthesis of geological knowledge and new data. Oceanologica Acta, 1, 335-358.

Guðlaugsson, S.T., Gunnarsson, K., Sand, M. and Skogseid, J. 1988. Tectonic and volcanic events at the Jan Mayen Ridge microcontinent. In: Morton, A.C. and Parson, L.M. (eds), Early Tertiary volcanism and the opening of the NE Atlantic, Geol. Soc. Special Publ., 39, 85-93.

Hinz, K., Mutter, J.C., Zehnder, C.M. and NGT Study Group. 1987. Symmetric conjugation of continent-ocean boundary structures along the Norwegian and East Greenland margins. Marine Petrol. Geol., 4, 166-187

Hinz, K. and Schluter, H. U. 1979. The North Atlantic - results of geophysical investigations by Federal Institute for Geosciences and Natural Resources on North Atlantic Continental Margins. Erdoel-Erdgas-Zeitschrift, 94, 271-280.

Johansen, B., Eldholm, O., Talwani, M., Stoffa, P.L. and Buhl, P. 1988. Expanding spread profile at the northern Jan Mayen Ridge. Polar Research.

Johnson, G. L. and Heezen, B. C. 1967. Morphology and evolution of the Norwegian-Greenland Sea. Deep Sea Res., 14, 755-771.

Larsen, H.C. 1988. A multiple and propagating rift model for the NE Atlantic. In: Morton, A.C. and Parson, L.M. (eds), Early Tertiary volcanism and the opening of the NE Atlantic, Geol. Soc. Special Publ., 39, 157-158.

Mutter, J.C., Buck, W.R. and Zehnder, C.M. 1988. Convective partial melting. 1. A model for the formation of thick basaltic sequences during the initiation of spreading. J. Geophys. Res., 93, 1031-1048.

Myhre, A. M., Eldholm, O. and Sundvor, E. 1984. The Jan Mayen Ridge: present status. Polar Res., 2, 47-59.

Mykkeltveit, S. 1980. A seismic profile in southern Norway. PAGEOPH, 118, 1310-1325.

Navrestad, T. and Jørgensen, F. 1979. Aeromagnetic investigations on the Jan Mayen Ridge. Norw. Petrol. Soc., NSS/9, 12p.

Nunns, A. G. 1983. Marine geophysical investigations in the Norwegian-Greenland Sea between latitude of 62°N and 74°N. Ph.D. thesis, University of Durham, England.

Ólafsson, I. 1983. The Jan Mayen Ridge and surrounding areas - A marine geophysical study. Cand real thesis, 127 pp University of Bergen, Norway.

Ólafsson, I. 1988. Deep crustal structure of the Møre margin from analysis of two-ship multichannel seismic data. Dr. scient thesis, 154 pp, University of Bergen, Norway.

Skogseid, J. and Eldholm, O. 1989. Vøring Plateau continental margin: seismic interpretation, stratigraphy and vertical movements. Submitted to Proc. Scientific Results ODP 104.

Skogseid, J. and Eldholm, O. 1987. Early Cenozoic crust at the Norwegian continental margin and the conjugate Jan Mayen Ridge. J. Geophys. Res., 92, 11471-11492.

Smythe, D.K, Chalmers, J.A., Skuce, A.G., Dobinson, A. and Mould, A.S. 1983. Early opening history of the North Atlantic - I. Structure and origin of the Faeroe-Shetland Escarpment. Geophys.J.R. Astr. Soc., 72, 373-398.

Talwani, M. and Eldholm, O. 1977. Evolution of the Norwegian-Greenland Sea. Geol. Soc. Am. Bull., 88, 969-999.

Talwani, M. and Udintsev, G. et al. 1976. Initial reports of the Deep Sea Drilling Project, Wasington, US, Government printing Office, 38, 1213-1242.

Vogt, P. R., Johnson, G. L. and Kristjánsson, L. 1980. Morphology and magnetic anomalies north of Iceland. J. Geophys. Res., 47, 67-80.

Vogt, P. R., Ostenso, N. A. and Johnson, G. L. 1970. Magnetic and bathymetric data bearing on seafloor spreading north of Iceland. J. Geophys. Res., 75, 903-920.

APPENDIX

Listing of all the sonobuoy solutions

sb 1, line jm-326-85, sp: 1-590

V (km/s)	Z (km)	T (sec)
1.48	.00	.00
1.48	1.55	2.10
1.85	1.55	2.10
1.85	2.57	3.20
3.00	2.57	3.20
3.00	3.25	3.65
5.50	3.25	3.65
5.50	3.93	3.90
5.05	3.93	3.90
5.05	4.44	4.10
5.40	4.44	4.10
5.40	5.79	4.60
7.00	5.79	4.60
7.00	7.89	5.20
7.50	7.89	5.20
7.50	9.39	5.60
8.00	9.39	5.60

sb 2, line jm-326-85, sp: 593-1020

V (km/s)	Z (km)	T (sec)
1.48	.00	.00
1.48	1.41	1.90
1.55	1.41	1.90
1.55	1.75	2.35
2.80	1.75	2.35
2.80	2.31	2.75
3.50	2.31	2.75
3.50	2.58	2.90
4.00	2.58	2.90
5.00	3.25	3.20
5.30	3.76	3.40
5.30	5.35	4.00

sb 3, line jm-326a-85, sp:1200-1880

V (km/s)	Z (km)	T (sec)
1.48	.00	.00
1.48	1.92	2.60
1.70	1.92	2.60
1.71	2.45	3.22
1.90	2.45	3.22
1.91	2.81	3.60
2.80	2.81	3.60
2.81	3.66	4.20
3.70	3.66	4.20
3.80	5.16	5.00
5.50	5.39	5.10
6.70	7.21	5.70
7.20	11.73	7.00

sb 5, line jm-226-85, sp:65-778

V (km/s)	Z (km)	T (sec)
1.48	.00	.00
1.48	2.10	2.84
1.55	2.10	2.84
1.56	2.30	3.10
2.20	2.30	3.10
2.21	3.46	4.15
3.00	3.53	4.20
4.10	5.64	5.40

4.11	6.46	5.80
6.50	8.28	6.50
7.00	9.97	7.00
7.20	17.07	9.00
7.50	17.07	9.00

sb 7, line jm-226-85, sp: 802-1387

V (km/s)	Z (km)	T (sec)
1.48	.00	.00
1.48	1.11	1.50
1.85	1.11	1.50
1.86	1.85	2.30
2.80	1.85	2.30
2.89	2.99	3.10
4.00	2.99	3.10
5.10	3.67	3.40
5.20	5.47	4.10
5.20	5.73	4.20
5.50	5.73	4.20
5.60	7.12	4.70
5.60	7.40	4.80

sb 10, line jm-226a-85, sp: 1525-2100

V (km/s)	Z (km)	T (sec)
1.48	.00	.00
1.48	1.04	1.40
1.60	1.04	1.40
1.75	1.75	2.25
2.10	1.94	2.45
2.75	2.06	2.55
3.10	2.35	2.75
3.10	2.43	2.80
3.50	3.17	3.25
4.75	3.27	3.30
5.90	7.12	4.75
6.20	7.27	4.80
6.75	13.09	6.60
7.00	13.09	6.60

sb 11, line jm-126-85, sp: 1-920

V (km/s)	Z (km)	T (sec)
1.50	.00	.00
1.50	.88	1.18
1.75	.88	1.18
1.75	1.24	1.58
2.35	1.24	1.58
2.35	1.96	2.20
3.40	1.96	2.20
4.60	3.35	2.90
4.90	4.07	3.20
5.25	4.95	3.55
5.50	11.00	5.80
6.80	11.00	5.80
7.60	15.31	7.00
8.00	15.31	7.00

sb 12, line jm-26-85, sp: 1453-1556

V (km/s)	Z (km)	T (sec)

1.48	.00	.00
1.48	.37	.50
1.80	.37	.50
2.80	1.61	1.60
3.60	1.77	1.70
3.90	1.96	1.80
4.50	1.96	1.80
4.80	2.43	2.00

sb 13, line jm-26-85, sp: 1559-2015

V (km/s)	Z (km)	T (sec)
1.48	.00	.00
1.48	.37	.50
1.80	.37	.50
2.30	1.29	1.40
2.30	1.40	1.50
3.30	1.40	1.50
4.10	1.77	1.70
5.10	2.80	2.15
5.60	4.01	2.60
5.70	4.57	2.80

sb 14, line jm-127-85, sp: 4445-5317

V (km/s)	Z (km)	T (sec)
1.48	.00	.00
1.48	.74	1.00
1.80	.74	1.00
1.80	.84	1.11
2.00	.84	1.11
2.00	.97	1.24
2.80	.97	1.24
2.80	1.47	1.60
4.70	1.47	1.60
4.70	3.16	2.32
6.20	3.16	2.32
6.20	9.55	4.38

sb 15, line jm-227-85, sp: 6896-7965

V (km/s)	Z (km)	T (sec)
1.48	.00	.00
1.48	.89	1.20
2.20	.89	1.20
2.20	1.88	2.10
4.40	1.88	2.10
4.40	3.64	2.90
5.10	3.64	2.90
5.10	4.91	3.40
5.80	4.91	3.40
6.50	7.68	4.30
7.00	7.68	4.30

sb 16, line jm-227-85, sp: 8081-9200

V (km/s)	Z (km)	T (sec)
1.48	.00	.00
1.48	.85	1.15
2.25	.85	1.15
2.40	1.14	1.40
3.25	1.42	1.60

3.80	2.48	2.20
5.00	2.48	2.20
5.00	3.98	2.80
5.20	3.98	2.80
5.80	8.10	4.30
6.00	8.10	4.30

sb 18, line jm-19b-85, sp: 1917-2619

V (km/s)	Z (km)	T (sec)
1.48	.00	.00
1.48	1.15	1.55
1.70	1.15	1.55
1.70	1.74	2.25
3.00	1.74	2.25
3.00	3.17	3.20
4.00	3.17	3.20
4.60	3.81	3.50
4.80	5.46	4.20
5.30	5.46	4.20
6.10	5.74	4.30
7.20	9.06	5.30
7.20	9.78	5.50

sb 19, line jm-14-85, sp: 45-790

V (km/s)	Z (km)	T (sec)
1.48	.00	.00
1.48	1.85	2.50
2.00	1.85	2.50
2.00	2.45	3.10
3.50	2.45	3.10
5.50	5.55	4.50
5.50	6.37	4.80

sb 20, line jm-14-85, sp: 884-1619

V (km/s)	Z (km)	T (sec)
1.48	.00	.00
1.48	.85	1.15
1.65	.85	1.15
1.65	1.02	1.35
3.80	1.02	1.35
4.00	1.21	1.45
4.12	1.52	1.60
4.25	1.93	1.80
4.62	2.60	2.10
5.00	3.80	2.60
5.00	4.80	3.00

sb 21, line jm-14-85, sp: 1643-2450

V (km/s)	Z (km)	T (sec)
1.48	.00	.00
1.48	2.04	2.75
1.70	2.04	2.75
1.70	2.47	3.26
1.80	2.47	3.26
2.20	2.91	3.70
2.40	3.25	4.00
2.70	3.25	4.00
3.60	4.27	4.65

4.20	5.44	5.25
4.20	5.54	5.30
4.50	5.54	5.30
6.40	7.43	6.00
7.30	10.17	6.80
7.30	10.90	7.00

sb 22, line jm-25-85, sp: 2514-3500

V (km/s)	Z (km)	T (sec)
1.48	.00	.00
1.48	1.65	2.23
1.80	1.65	2.23
1.81	1.90	2.51
2.00	1.90	2.51
2.01	2.30	2.91
2.25	2.30	2.91
2.26	2.80	3.35
3.20	2.80	3.35
3.21	3.81	3.98
4.50	4.04	4.10
6.80	5.15	4.50
6.90	5.50	4.60
7.00	5.84	4.70

sb 23, line jm-25-85, sp: 5929-6800

V (km/s)	Z (km)	T (sec)
1.48	.00	.00
1.48	1.05	1.42
1.70	1.05	1.42
1.80	1.62	2.07
2.50	1.62	2.07
2.70	2.36	2.64
3.30	2.36	2.64
3.51	3.14	3.10
4.10	3.14	3.10
4.30	4.40	3.70
4.50	4.40	3.70
5.10	4.76	3.85
5.70	5.98	4.30
6.70	7.52	4.80
6.80	8.20	5.00

sb 24, line jm-2-85, sp: 82-776

V (km/s)	Z (km)	T (sec)
1.48	.00	.00
1.48	.48	.65
2.50	.48	.65
2.51	1.67	1.60
4.70	1.67	1.60
6.10	4.89	2.80
6.20	8.58	4.00

sb 25, line jm-2-85, sp: 836-1700

V (km/s)	Z (km)	T (sec)
1.48	.00	.00
1.48	.33	.45
1.75	.33	.45
2.10	.67	.80
2.10	.77	.90

2.80	.77	.90
3.70	1.34	1.25
3.90	1.81	1.50
4.60	2.87	2.00
5.90	4.83	2.75
7.50	7.33	3.50

sb 26, line jm-2-85, sp: 1756-2800

V (km/s)	Z (km)	T (sec)
1.48	.00	.00
1.48	2.00	2.70
1.80	2.00	2.70
1.80	2.40	3.15
2.40	2.40	3.15
2.40	2.94	3.60
4.20	3.18	3.75
4.90	3.75	4.00
5.50	4.53	4.30
6.50	6.63	5.00
6.70	7.29	5.20
7.10	7.98	5.40
7.10	11.53	6.40

sb 27, line jm-24b-85, sp: 1400-2240

V (km/s)	Z (km)	T (sec)
1.48	.00	.00
1.48	2.18	2.95
1.80	2.18	2.95
2.10	2.67	3.45
2.30	2.67	3.45
2.40	3.08	3.80
4.00	3.47	4.05
6.00	5.08	4.70
7.00	7.02	5.30
7.20	8.80	5.80

sb 28, line jm-124-85, sp: 4851-5600

V (km/s)	Z (km)	T (sec)
1.48	.00	.00
1.48	2.50	3.38
1.65	2.50	3.38
1.65	3.05	4.05
2.45	3.05	4.05
2.45	3.95	4.78
3.30	3.95	4.78
3.30	4.24	4.96
3.60	4.24	4.96
3.60	4.94	5.34
4.12	5.52	5.65
5.12	6.33	6.00
7.10	7.84	6.50
7.10	8.20	6.60

sb 29, line jm-224-85, sp:6332-6948

V (km/s)	Z (km)	T (sec)
1.48	.00	.00
1.48	2.44	3.30
1.85	2.44	3.30

1.85	2.63	3.50
1.95	2.63	3.50
1.95	3.02	3.90
2.30	3.02	3.90
2.30	3.59	4.40
2.90	3.59	4.40
3.40	4.69	5.10
4.40	5.08	5.30
6.80	7.01	6.00
6.80	7.69	6.20

sb 30, line jm-224-85, sp: 8131-8900

V (km/s)	Z (km)	T (sec)
1.48	.00	.00
1.48	2.37	3.20
1.75	2.37	3.20
1.75	2.85	3.75
1.90	2.85	3.75
1.90	3.37	4.30
3.00	3.79	4.65
3.20	3.79	4.65
3.30	4.93	5.35
4.00	4.93	5.35
6.50	7.12	6.20
6.60	7.45	6.30

sb 32, line jm-11a-85, sp: 11-806

V (km/s)	Z (km)	T (sec)
1.48	.00	.00
1.48	3.18	4.30
1.75	3.18	4.30
1.75	3.88	5.10
3.30	4.49	5.60
3.40	4.83	5.80
3.40	5.00	5.90
5.00	5.00	5.90
6.50	7.00	6.60
7.30	10.79	7.70
7.50	10.79	7.70

sb 33, line jm-11a-85, sp: 807-1520

V (km/s)	Z (km)	T (sec)
1.48	.00	.00
1.48	2.66	3.60
1.80	2.66	3.60
1.80	3.47	4.50
2.50	3.47	4.50
2.60	3.98	4.90
3.10	3.98	4.90
3.20	4.46	5.20
4.30	4.46	5.20
6.60	7.41	6.30
7.30	14.01	8.20
7.50	14.01	8.20

sb 35, line jm-11a-85, sp: 2615-3100

V (km/s)	Z (km)	T (sec)
1.48	.00	.00

1.48	2.15	2.90
1.55	2.15	2.90
1.60	2.38	3.20
1.80	2.38	3.20
1.90	2.66	3.50
2.60	2.66	3.50
2.70	4.65	5.00
4.50	4.82	5.10
4.80	5.75	5.50
4.80	6.23	5.70

sb 38, line jm-11a-85, sp: 3308-3788

V (km/s)	Z (km)	T (sec)
1.48	.00	.00
1.48	2.22	3.00
1.60	2.22	3.00
1.70	2.63	3.50
3.80	2.63	3.50
4.95	2.85	3.60
5.00	3.10	3.70
2.60	3.10	3.70
2.70	4.56	4.80
5.40	4.56	4.80
5.50	7.28	5.80
6.00	7.28	5.80

sb 39, line jm-8-85, sp: 842-1550

V (km/s)	Z (km)	T (sec)
1.50	.00	.00
1.50	2.10	2.80
1.70	2.10	2.80
1.70	2.69	3.50
3.20	2.69	3.50
3.20	4.30	4.50
4.80	4.30	4.50
4.80	4.53	4.60
4.20	4.53	4.60
4.20	5.79	5.20
4.50	5.79	5.20

sb 40, line jm-8-85, sp: 1568-1800

V (km/s)	Z (km)	T (sec)
1.48	.00	.00
1.48	.74	1.00
1.70	.74	1.00
1.70	1.00	1.30
3.40	1.00	1.30
4.08	1.83	1.75
4.10	1.94	1.80
4.80	1.94	1.80
5.00	2.92	2.20

sb 41, line jm-8-85, sp: 2341-3050

V (km/s)	Z (km)	T (sec)
1.50	.00	.00
1.50	1.57	2.09
1.95	1.57	2.09
1.95	2.06	2.60

1.80	2.06	2.60
1.80	2.81	3.43
4.94	4.16	4.30
6.12	6.09	5.00
7.20	7.75	5.50
7.20	9.55	6.00

sb 42, line jm-8-85, sp: 3068-3987

V (km/s)	Z (km)	T (sec)
1.48	.00	.00
1.48	2.55	3.45
1.85	2.55	3.45
1.85	2.80	3.72
1.90	2.80	3.72
1.90	3.11	4.04
2.55	3.11	4.04
2.55	3.81	4.59
3.80	3.81	4.59
4.30	4.13	4.75
6.60	6.82	5.75
7.20	8.37	6.20
7.40	9.46	6.50
7.40	15.01	8.00

sb 43, line jm-129-85, sp: 1-701

V (km/s)	Z (km)	T (sec)
1.48	.00	.00
1.48	2.15	2.90
1.90	2.15	2.90
1.90	2.72	3.50
2.90	2.72	3.50
4.40	3.44	3.90
5.40	3.68	4.00
5.50	3.95	4.10
2.60	3.95	4.10
2.70	5.14	5.00
4.80	5.14	5.00
4.90	8.05	6.20
6.10	8.05	6.20
6.20	11.74	7.40
7.00	11.74	7.40

sb 44, line jm-128-85, sp 5872-6800

V (km/s)	Z (km)	T (sec)
1.48	.00	.00
1.48	1.81	2.45
1.65	1.81	2.45
1.65	2.18	2.90
2.35	2.18	2.90
2.35	2.89	3.50
2.60	2.89	3.50
3.40	3.19	3.70
4.25	4.14	4.20
4.90	4.94	4.55
6.10	7.54	5.50
6.20	9.08	6.00
6.90	9.08	6.00
7.00	11.86	6.80

sb j1, line j-1-79, sp: 2056-2775

V (km/s)	Z (km)	T (sec)
1.48	.00	.00
1.48	2.27	3.07
1.60	2.27	3.07
1.60	2.54	3.40
2.06	2.90	3.80
2.20	3.22	4.10
2.20	3.33	4.20
2.75	3.33	4.20
3.00	3.90	4.60
3.60	4.40	4.90
3.62	4.58	5.00
5.60	5.26	5.30
6.20	7.62	6.10
7.00	7.62	6.10

sb-j2, line j-2-79, sp: 1571-2328

V (km/s)	Z (km)	T (sec)
1.48	.00	.00
1.48	1.92	2.60
1.90	1.92	2.60
1.95	3.42	4.15
2.40	3.42	4.15
3.30	3.56	4.25
4.10	5.12	5.10
4.11	5.33	5.20
4.90	5.44	5.25
5.60	7.41	6.00
6.40	8.31	6.30
6.90	9.30	6.60
7.20	16.00	8.50
8.00	16.00	8.50

sb-j6, line j-6-79, sp: 1093-1780

V (km/s)	Z (km)	T (sec)
1.48	.00	.00
1.48	1.18	1.40
1.90	1.18	1.40
1.91	1.84	2.10
2.90	1.84	2.10
3.20	3.22	3.00
4.20	3.22	3.00
5.30	7.47	4.80
6.60	8.95	5.30
7.30	14.85	7.00
8.00	14.85	7.00